Bacterial prey food characteristics modulate community growth response of freshwater bacterivorous flagellates

Šimek, Karel ; Grujčić, Vesna ; Hahn, Martin W ; Horňák, Karel ; Jezberová, Jitka ; Kasalický, Vojtěch ; Nedoma, Jiří ; Salcher, Michaela M ; Shabarova, Tanja

Abstract: Different bacterioplankton species represent different food quality resources for heterotrophic nanoflagellate (HNF) communities, potentially affecting HNF growth, community dynamics and carbon flow to higher trophic levels. However, our knowledge of such dynamics is still very limited. Here, we describe the results of 11 experiments with natural HNF communities from distinct seasonal phases in two freshwater habitats. The HNF communities were released from predation pressure of zooplankton and incubated with 16 distinct ecologically relevant prey bacterial strains from important Betaproteobacteria genera (Limnohabitans, Polynucleobacter, and Methylopumilus) and one Actinobacteria strain from the Luna 2 cluster. We observed remarkable prey- and season-specific variability in community HNF growth parameters, i.e., doubling time, volumetric gross growth efficiency (GGE), and length of lag phase. All strains, except for the actinobacterium, supported rapid HNF population growth with an average doubling time of 10 h and GGE of 29%. Our analysis revealed that 59% of the variability in flagellate GGE data was explained by the length of lag phase after prey amendments. This indicates a considerable "adaptation time," during which the predator communities undergo compositional shifts toward flagellate bacterivores best adapted to grow on the offered prey. Importantly, the rapid HNF growth detected on various bacteria tightly corresponds to doubling times reported for fast growing bacterioplankton groups. We propose a conceptual model explaining the tight linkages between rapid bacterial community shifts and succeeding HNF community shifts, which optimize prey utilization rates and carbon flow from various bacteria to the microbial food chain.

DOI: https://doi.org/10.1002/lno.10759

Bacterial prey food characteristics modulate community growth response of freshwater bacterivorous flagellates

Karel Šimek[1,2], Vesna Grujčić[1,2], Martin W. Hahn[3], Karel Horňák[1,♦], Jitka Jezberová[1], Vojtěch Kasalický[1], Jiří Nedoma[1], Michaela M. Salcher[1♦], Tanja Shabarova[1]

[1] Biology Centre of the Czech Academy of Sciences, Institute of Hydrobiology, Na Sádkách 7, 37005 České Budějovice, Czech Republic

[2] University of South Bohemia, Faculty of Science, Branišovská 31, 37005 České Budějovice, Czech Republic

[3] Research Department for Limnology, University of Innsbruck, Mondsee, Austria

♦ Present address: Limnological Station, Department of Plant and Microbial Biology, University of Zurich, Kilchberg 8802, Switzerland

Running head: Bacterial prey quality controls flagellate growth

Keywords: Flagellate growth characteristics, gross growth efficiency, food quality of bacteria, predator-prey interactions, freshwater plankton, ecological implications

Written as an Research article in *Limnology and Oceanography*

Correspondence

Karel Šimek

Biology Centre CAS, Institute of Hydrobiology, Na Sádkách 7, CZ-37005 České Budějovice, Czech Republic

Phone number: +420 387775873; FAX number: +420 385310248; e-mail: ksimek@hbu.cas.cz

Abstract. Different bacterioplankton species represent different food quality resources for heterotrophic nanoflagellate (HNF) communities, potentially affecting HNF growth, community dynamics and carbon flow to higher trophic levels. However, our knowledge of such dynamics is still very limited. Here we describe the results of 11 experiments with natural HNF communities from distinct seasonal phases in two freshwater habitats. The HNF communities were released from predation pressure of zooplankton and incubated with 16 distinct ecologically relevant prey bacterial strains from important *Betaproteobacteria* genera (*Limnohabitans*, *Polynucleobacter* and *Methylopumilus*) and one *Actinobacteria* strain from the Luna 2 cluster. We observed remarkable prey- and season-specific variability in community HNF growth parameters, i.e. doubling time, volumetric gross growth efficiency (GGE), and length of lag phase. All strains, except for the actinobacterium, supported rapid HNF population growth with an average doubling time of 10 h and GGE of 29%. Our analysis revealed that 59% of the variability in flagellate GGE data was explained by the length of lag phase after prey amendments. This indicates a considerable "adaptation time", during which the predator communities undergo compositional shifts towards flagellate bacterivores best adapted to grow on the offered prey. Importantly, the rapid HNF growth detected on various bacteria tightly corresponds to doubling times reported for fast growing bacterioplankton groups. We propose a conceptual model explaining the tight linkages between rapid bacterial community shifts and succeeding HNF community shifts, which optimize prey utilization rates and carbon flow from various bacteria to the microbial food chain.

Introduction

In freshwater systems, the trophic interactions of protists and prokaryotes regulate the flow of dissolved organic carbon and limiting nutrients to higher trophic levels (Jürgens and Matz 2002; Sherr and Sherr 2002). Heterotrophic nanoflagellates (HNF), ciliates, and in nutrient poor systems, mixotrophic flagellates (e.g. Domaizon et al. 2003; Weisse et al. 2016),

50 are considered to be major protistan bacterivores. Trophic interactions are well characterized
51 from the perspective of the top-down control of bacteria. Various size-related grazing-resistant
52 strategies, but also non-morphological traits of prokaryotes such as motility, cell surface
53 properties, and the effect of bacterial toxicity on their vulnerability to protistan grazing are
54 well documented (Hahn and Höfle 2001; Jürgens and Matz 2002). However, how these
55 interactions may regulate consumer success (Boenigk and Arndt 2002; Corno et al. 2013;
56 Chrzanowski and Foster 2014) and, in turn, also the community composition of the
57 bacterivores (Arndt et al. 2000; Šimek et al. 2013) is much less understood.
58 The amounts, composition, and temporal dynamics of organic and inorganic resources
59 differ remarkably both seasonally and among various freshwater bodies. These resources
60 ultimately modulate the growth and population dynamics of various planktonic prokaryotes
61 (Eiler and Bertilsson 2007; Salcher et al. 2013; Salcher 2014). Detailed insights into
62 bacterioplankton community composition and substrate preferences are increasingly
63 becoming available (e.g. Newton et al. 2011; Salcher et al. 2013). While these represent useful
64 "snapshots" of the community at a given time point, they are not informative regarding
65 turnover rates of major bacterioplankton groups. Such investigations require fine temporal
66 resolution reflecting typical doubling times of planktonic prokayotes as well as protistan
67 predators (Eckert et al. 2012; Šimek et al. 2014). Thus, the currently available data on
68 bacterioplankton composition in situ cannot be translated into growth rates and carbon fluxes
69 from the bacteria to the grazer food chain.
70 It has been suggested that the driving force for high bacterial production in pelagic
71 environments is mediated by frequent resource shifts supporting short-lived peaks of rapidly
72 growing bacterial lineages (Eckert et al. 2012, 2013; Salcher 2013). For instance, some
73 *Betaproteobacteria* and *Flavobacteria* respond to sudden pulses in algal-derived organic
74 carbon with very short doubling times from several hours to days (Zeder et al. 2009; Salcher

et al. 2011; Neuenschwander et al. 2015). These short-lived bacterial peaks are rapidly succeeded by peaks of bacterivorous HNF (Eckert et al. 2012; Šimek et al. 2014). Thus, it has been hypothesized that small grazers rapidly adapt to the shifts in prey communities owing to their growth potential in situ (Šimek et al. 2006; Weisse et al. 2016). Pelagic HNF populations are usually severely top-down controlled by zooplankton grazing (e.g. Jürgens et al. 1996), while bacterial concentrations in meso-eutrophic systems do not appear to be a key factor limiting HNF growth (Jürgens 1992; Gasol and Vaqué 1993). In contrast, the trophic position of bacteria at the bottom of the food chain suggests that they are more strongly resource-limited (McQueen et al. 1986).

Different bacterial strains appear to have different nutritional value to consumers (Boenigk et al. 2006; Tarao et al. 2009; Šimek et al. 2013; Chrzanowski and Foster 2014) and this characteristic may vary even for the same prey during different seasonal phases within the same ecosystems (Grujčić et al. 2015). Moreover, the same bacterial species may not have similar nutritional quality for all members of the flagellate community (Chrzanowski and Foster 2014). Thus, seasonal shifts in prey availability likely induce very different, prey-specific growth responses of the HNF grazers, measured as growth rate and gross growth efficiency (GGE). These findings suggest that shifts in bacterial community structure (Newton et al. 2011; Salcher et al. 2013), with concomitant shifts in the quality of bacteria as food, likely cascades upward, inducing shifts in the bacterivore community (Šimek et al. 2013; Chrzanowski and Foster 2014). Many different methods to study HNF bacterivory have been proposed; however, none are appropriate for assessing the specific role of a naturally abundant prey in carbon flow dynamics (Montagnes et al. 2008). So far only a few experimental studies have focused on the growth responses of natural HNF assemblages to bacterial prey amendments using strains of relevant prokaryotic taxa that are those originating from the same systems as the consumers (Šimek et al. 2013; Grujčić et al. 2015). The lack of such data

severely limits the possibility to generalize preliminary evidence on a tight coupling between prey community shifts and variable growth responses of HNF associated with very rapid shifts in the grazer community (Šimek et al. 2013), the phenomena that can be modulated by seasonally evolving trophic structure of plankton environments (e.g. Grujčić et al. 2015).

Thus in a large series of 11 flagellate predator-bacterial prey manipulation experiments, we tested the hypothesis that HNF communities rapidly respond to prey availability shifts in prey-specific fashion, with growth rates comparable to those of pelagic bacteria. Natural HNF communities in plankton samples, originating from different seasonal phases in two distinct ecosystems, and an axenic culture of *Poterioochromonas* sp. were used as flagellate bacterivores. Treatments with flagellate grazers were manipulated by the addition of 16 different strains from relevant and abundant bacterioplankton taxa (Newton et al. 2011; Jezbera et al. 2012). The aim of this study was to investigate general net effects of bacterial prey quality, specifically, the maximum growth rate, the volumetric GGE, and the length of the lag phase in different flagellate taxa. Based on our results and the existing literature we propose a conceptual model explaining the tight linkages between the rapid shifts in the bacterial community and the consequent shifts in HNF community, that optimize prey utilization rates and biomass transfer from various bacteria to higher trophic levels.

Materials and methods

Experimental organisms

For the bacterial prey manipulation experiments we used 16 representative strains (*see* Table 1 for the full list of the strains, their cell size, morphology, and origin) from several important lineages of planktonic bacteria:

(i) Genus *Limnohabitans* of *Betaproteobacteria* - one strain from the lineage LimA (Rim8), one strain from the lineage LimB (Rim11), and nine strains of diverse size and morphology from the lineage LimC (II-D5^T, II-B4^T, 2KL-27, 2KL-1, 2KL-3, T6-5, Rim28, Rim47, and

15K). Two of the strains, designated II-B4^T and II-D5^T (16S rRNA gene accession numbers FM165536 and FM165535, respectively) represent type strains of the species *L. parvus* and *L. planktonicus* (Kasalický et al. 2010) while the other *Limnohabitans* strains represent so far undescribed species. Reconstructions of the phylogenetic positions of all these strains based on 16S rRNA gene and ITS sequences were presented elsewhere (Kasalický et al. 2013). Seven out of 11 *Limnohabitans* strains were isolated from the surface layer of the freshwater mesoeutrophic Římov Reservoir in South Bohemia (48°50'56"N, 14°29'26"E), 3 strains from the mesoeutrophic Klíčava Reservoir in Central Bohemia (50°3'58"N, 13°55'55"E), and one strain from the eutrophic Lužnice pond T6 in South Bohemia (48°50'0.453"N, 14°55'40.324"E, *see* Table 1). All strains from the B and C lineages of the genus *Limnohabitans* belong to the R-BT065 subcluster of *Betaproteobacteria* (for the probe targets, *see* Šimek et al. 2001), while the lineage Lim A is detectable in environmental samples with a double hybridization approach using a novel 23S rRNA FISH-probe (Shabarova et al. 2017).

(ii) Genus *Polynucleobacter* of *Betaproteobacteria* - we used two undescribed strains from PnecC lineage - czRimov8-C6 (accession number FN429658, Jezbera et al. 2011) and czRimov-FAMC1, isolated from the Římov Reservoir (Table 1) with identical 16S rRNA sequences. Furthermore, one *Polynucleobacter* strain from the PnecD lineage, *P. cosmopolitanus* (MWH-MoIso2^T), isolated from Lake Mondsee in Austria (Hahn et al. 2010), was used in our experiments.

(iii) Genus *Methylopumilus*, *Methylophilaceae, Betaproteobacteria* – we used one strain *Ca. M. turicensis* (MMS-10A-171) isolated from Lake Zurich in Switzerland (Salcher et al. 2015).

(vi) Luna 2 cluster of *Actinobacteria* – we used one undescribed strain (MWH-Wo1) isolated from Lake Wolfgangsee (Hahn and Pöckl 2005).

The mixotrophic flagellate predator *Poterioochromonas* sp. strain DS was isolated from Lake Constance (accession number of 18S rRNA gene sequence AM981258, Tarao et al.

2009). The axenic flagellate culture was maintained in dim light and fed twice a month with heat-killed bacteria (60°C, *L. planktonicus* strain; pelletized aliquots stored frozen in -20°C) as described previously (Hahn et al. 1999).

Experimental design and sampling

The majority of the strains used as prey for flagellates were isolated from our major study site (the Římov Reservoir, Table 1). Before each experiment, the bacteria were pre-grown in the nutrient rich liquid 3 g l^{-1} NSY medium (Hahn et al. 2004) to avoid possible effects of nutrient-deficient prey on flagellates selectivity and grazing and thus to standardize the experimental start point regarding prey food quality related to the nutrient content.

Altogether 11 experiments (for an overview *see* Table 2) were conducted during 2011-2015, spanning different seasonal phases at two natural sites – the Římov Reservoir and oligomesotrophic sandpit Lake Cep (48°92'49.24"N, 14°88'68.11"E, South Bohemia, Czech Republic). We used natural HNF communities (experiments IA, II-XI; Table 2) or the axenic *Poterioochromonas* culture (experiment IB) to examine effects of different food quality of different bacteria (Table 1) on growth parameters of the flagellate communities. Both grazer populations (HNF and *Poterioochomonas* sp.) were amended in parallel by adding exactly the same total bacterial biovolume of the bacterial strains (experiments IA and IB, Table 2).

During the exponential growth phase, bacterial cells (50 ml) were concentrated by centrifugation at 5000 g and subsequently re-suspended into 50 ml of 0.2-μm filtered and sterilized water from the Římov Reservoir (experiments I-III, V, and VII-XI, *see* Table 2), or water from Lake Cep (experiments IV and VI). The cultures were kept on a shaker overnight to facilitate even re-suspension of cells and adaptation to the reservoir or lake water as detailed elsewhere (Šimek et al. 2013; Grujčić et al. 2015). *Ca. M. turicensis* was grown in 2 l setups in autoclaved water from the Římov Reservoir amended with 1 mM methanol, 100 μM methylamine, and concentrated by centrifugation. Prior to being added to experimental

175 treatments, bacteria were enumerated via fluorescence microscopy as described below.

176 All experiments with natural HNF communities from the two planktonic systems (Table
177 2) as well as with the *Poterioochromonas* culture were carried out in a very similar fashion. A
178 10-liter water sample from the Římov Reservoir or Lake Cep was collected and then gravity-
179 filtered through 5-μm pore-size, 147-mm diameter filters (for more details *see* Šimek et al.
180 2013 and Grujčić et al. 2015). The HNF in filtered water were thus released from zooplankton
181 predation and the samples were pre-incubated for 10 h to recover from the handling shock in
182 samples with relatively high HNF abundance (1–4 × 10^3 ml^{-1}) or up to 30 h in samples from
183 May and October with low HNF abundance (< 0.7 × 10^3 ml^{-1}; Table 2). The longer pre-
184 incubation resulted in a marked increase in HNF numbers, yielding time zero abundance
185 within the range of 1.5 to 3.5 × 10^3 ml^{-1}. Moreover, during the pre-incubation period the
186 abundance of the natural background bacteria decreased to levels of ca. 1 × 10^6 ml^{-1}, and the
187 majority of remaining bacteria were either small flocks or filaments (i.e. likely HNF grazing-
188 resistant morphotypes). After the pre-incubation, triplicate treatments of 250–500 ml of the 5-
189 μm filtrates were manipulated by addition of the respective bacterial strains. The scheme of
190 major steps of the experimental setup has been described elsewhere (Fig. 1 in Šimek et al.
191 2013). Small ciliates may in some cases pass through 5-μm pore-size filters (Nakano et al.
192 2001) and prey upon flagellates. However, we checked all samples from the exponential phase
193 used to calculate HNF growth parameters (largely time points between 12 to 70 h) and did not
194 find any ciliates.

195 Six days before starting the experiment 1B (Table 2), we stopped the feeding of the axenic
196 *Poterioochromonas* culture by heat killed food bacteria. Notably, during this period almost all
197 fed bacteria were consumed by the flagellate (approximately 5 × 10^3 flagellates ml^{-1}) and thus
198 they could not interfere substantially with bacterial food amendments. Moreover, the
199 flagellate culture was further diluted by the bacteria-free inorganic IBM medium (Hahn et al.

2004) to yield a starting flagellate concentration of 1×10^3 ml^{-1}. Six bacterial prey types were then added to the flagellate culture (experiment IB) and their same biovolume also to the natural HNF community (experiment IA). The differences in the numbers of bacteria added in particular experiments, ranging from 15 to 45×10^6 cells ml^{-1}, reflect the fact that the prey bacteria differed markedly in mean cell volume and morphology (Table 1). The initial cell number of each bacterial strain added was set to yield approximately the same initial biovolume for all strains within the same experiment. This biovolume ($1.5–5.5 \times 10^6$ μm^3 ml^{-1}) represented 10–20-fold the background bacterial biomass present in the pre-incubated HNF solution. A 5-μm filtrate containing the same starting HNF community but with no bacteria added was used as control. Thus the differences in growth responses of HNF in the amended treatments could be attributed to the effects induced by the prey added. Experiments were run for 66–100 h (in case of a longer lag phase) to cover the HNF exponential growth phase, usually till their numbers started to decrease (for details *see* Suppl. Information, Figs. S1–S8). All treatments were incubated in the dark at 18°C (within ± 3°C of the in situ temperature; Table 2), and subsamples were taken aseptically at 12–24 h intervals. At time 0 h, 24 h and at the time point corresponding to exponential growth phase of HNF communities, additional samples were collected for fluorescence in situ hybridization (CARD-FISH, *see* below).

Timing of the experiments fell into 4 different plankton successional phases: April (spring phytoplankton bloom), May (clear water phase), August (late summer phytoplankton bloom), and October (decaying algal bloom phase). Since many strains were used repeatedly in the different seasonal phases at both sites (Table 2) we also tested how the same bacterial strain affects the growth of temporally different HNF communities. For such statistical testing the data from the same prey amendments falling into the same seasonal phase were pooled together from both study sites (for details *see* Suppl. Information Table S1).

The impacts of prey amendments on the HNF community composition in experiment marked as IA in Table 2 have been evaluated separately in Šimek et al. (2013) and the comparisons of season- and site-specific aspects of HNF growth responses to addition of 3 identical strains in experiments marked as III-VI (Table 2) are detailed in Grujčić et al. (2015). However, the data from these experiments were used also in this comprehensive study in a broader context to unveil the overall trends of HNF growth responses and their possible community shifts induced by prey amendments with a far broader variety of relevant planktonic bacteria used, moreover, across different plankton seasonal phases.

Bacterial abundance and sizing

In experiments IA, IB and II, bacterial abundance was quantified via flow cytometry in samples stained with the fluorochrome Syto13 (Molecular Probes, Eugene, OR, USA) using the FACScalibur flow cytometer (Becton Dickinson, Franklin Lakes, NJ, USA) as detailed in Gasol and Del Giorgio (2000). However, after approximately 60 h of the experiments with growing abundance of grazers, enhanced proportions of flocks and filaments (apparently developing from natural background bacterioplankton cells) appeared in the samples and thus bacteria were counted via epifluorescence microscopy (Šimek et al. 2001). This also allowed accurate quantification of bacterial cells in small bacterial aggregates. In the follow up experiments, i.e. III - XI, bacterial abundance was quantified only via the microscopy. Bacteria (> 200 cells per sample) were sized by using the semiautomatic image analysis systems (NIS-Elements 3.0, Laboratory Imaging, Prague, Czech Republic).

Heterotrophic flagellate enumeration, growth and cell size

Subsamples (1–5 ml) were stained with DAPI (4',6-diamidino-2-phenylindole) and HNF abundance (eukaryotic cells with a visible nucleus, flagella, and typical cell shape), was determined via epifluorescence microscopy as described elsewhere (Šimek et al. 2001). To calculate mean volumes of HNF cells (approximated to prolate spheroids), lengths and widths

249 of > 50 cells in triplicate treatments were measured manually on-screen with a built-in tool
250 established in the software NIS-Elements 3.0 (LIM, Prague, Czech Republic). Estimates of
251 GGE of HNF as percent based on cellular biovolume were calculated as the ratio between
252 bacterial biovolume introduced and net HNF biovolume yield in the treatment (Šimek et al.
253 2013), thus representing the volumetric GGE, not carbon-based GGE values. The maximum
254 HNF growth rate was calculated using ln-transformed data on HNF abundance with linear
255 regression as the slope of the best-fit line. The length of lag phase was calculated as the period
256 from the time zero to the intercept between the best-fit line of HNF growth and the zero-time
257 level of HNF abundance (Šimek et al. 2013). To illustrate the data selection and calculations
258 used, commented examples of time-course changes in flagellate abundance, biovolume and
259 bacterial biovolume for the experiment IB are given in Fig. 1.

260 **Catalyzed reporter deposition fluorescence in situ hybridization (CARD-FISH)**

261 The CARD-FISH protocol (Pernthaler et al. 2002) and oligonucleotide probes
262 (ThermoHybaid, Ulm, Germany) were employed to target the following bacterial lineages: the
263 R-BT065 cluster (probe R-BT065, Šimek et al. 2001), that includes all *Limnohabitans* strains
264 used from the lineage LimB and LimC (Kasalický et al. 2013); the LimA lineage of the
265 *Limnohabitans* genus (probe LimAE-1435, Shabarova et al. 2017); the entire cluster of
266 *Polynucleobacter* (probe PnecABCD-445, Hahn et al. 2005); the PRD01a001B lineage of
267 *Methylophilaceae*, *Betaproteobacteria* (probe PRD-732, targeting *M. turicensis*, Salcher et al.
268 2015); and the entire *Actinobacteria* phylum (probe HGC69a). We examined proportions of
269 the probe-targeted bacteria in plankton of the study sites at the time zero (t_0), and in all
270 experimental treatments at times t_{24} h and during HNF exponential growth phase (mostly
271 within t_{48} to t_{66} h). Moreover, for verifying the assumed bacteria-flagellates carbon transfer,
272 the presence of the prey bacteria in HNF food vacuoles was detected (Jezbera et al. 2005).

273 **Phosphorus and Chl *a* concentrations**

Water used for experiments was analyzed to determine concentrations of (Table 2): Dissolved reactive phosphorus (Murphy and Riley 1962), total phosphorus (the molybdate method detailed in Kopáček and Hejzlar 1993), and chlorophyll *a* determined spectrophotometrically after the extraction with acetone (Lorenzen 1967).

Statistical analysis

Statistical analyses were performed with Statistica v. 13 (Dell Inc.). Using an appropriate design of ANOVA we tested differences in growth parameters of flagellates (growth rate, volumetric GGE, and length of lag phase) associated with grazer type (natural planktonic HNF community versus the mixotrophic flagellate *Poterioochromonas* sp.), season (April, May, August, or October), and bacterial strain or lineage used as prey, or a combination of these factors. We used one-way ANOVA for testing of effects of single factors, two-way ANOVA for testing effects of combinations of two factors; in the case of incomplete design we used Effective hypothesis decomposition. The Unequal N HSD multiple comparison post-hoc tests were used to determine differences between groups.

Results

Environmental relevance of bacterial strains used as prey for natural HNF communities

Sixteen different bacterial strains (Table 1) were used in prey-amendment experiments (an overview in Table 2). We used mainly strains from different lineages of *Limnohabitans* and *Polynucleobacter* genera isolated from the epilimnion of Římov reservoir (9 bacterial strains out of 16, Table 1), or from the *Limnohabitans* lineages detected at this site by different methods over a seasonal cycle (Šimek et al. 2008, 2014, Jezberová et al. 2017, in press).

Environmental relevance of *Limnohabitans* bacteria was tested with the use of the R-BT065 FISH probe, targeting the R-BT cluster of the genus *Limnohabitans* (covering the Lim B, C, D, and E lineages, Kasalický et al 2013). In the original samples used for experiments

298 (Table 2) and in seasonal studies of the reservoir bacterioplankton (Šimek et al. 2008, 2014)
299 we found the following relative proportions of *Limnohabitans* bacteria (as % of total bacteria;
300 mean and range of values): (i) the spring bloom phase in April (14.1%; 8.4–17.5%); (ii) clear
301 water phase in May (9.6%, 7.2–11.8%); (iii) summer phytoplankton bloom in August (6.1%,
302 3.5–9.4%); and October period (5.9, 3.5–9.4%). In experiments IV and VI, conducted in April
303 and May solely with *Limnohabitans* isolates in Lake Cep (Table 2), the R-BT cluster
304 accounted for 10.2% and 8.3% of total pelagic bacteria in the lake, respectively.
305 The strains from the *Polynucleobacter* C lineage were used in April and August 2014
306 (experiments IX and X, Table 2) when this lineage accounted for 6.6% and 3.0% of total
307 bacteria in the reservoir plankton, respectively. The probes targeting the LimA lineage of the
308 genus *Limnohabitans* (probe LimAE-1435) and *M. turicensis* (probe PRD-732), whose
309 representative strains were used only in May 2015 experiment (XI, Table 2), showed that both
310 these bacterial phylotypes formed approximately 2% of total reservoir bacterioplankton.
311 **Growth responses of different flagellate grazers**
312 We employed a virtually identical experimental design in all of the experiments
313 (overview in Table 2) to estimate maximum growth rate (or doubling time), volumetric GGE
314 and length of lag phase after prey amendment of the treatment. Examples of calculations of
315 the parameters are given in Fig. 1 (*see* 5 prey-amended treatments and the explanatory text),
316 showing time course changes in abundance and biovolumes of the *Poterioochromonas* sp.
317 flagellate related to the rates of decrease in biovolumes of six different prey bacteria added
318 (experiment IB, Table 2). The data for the strain MWH-Wo1 (*Actinobacteria*) and control
319 treatments are not plotted in Fig. 1, as no flagellate growth was detected and thus the growth
320 parameters could not be calculated (*see* also Fig. 2 and Suppl. Information Fig. S1).
321 To compare the growth responses of the single species flagellate culture in comparison to
322 a mixed community of planktonic HNF (experiments IA and IB in Table 2), the same six prey

items were simultaneously added at the same time point to a natural HNF community sample collected from the Římov Reservoir (Fig. 2). The comparison of growth parameters showed significant differences ($p < 0.05$, two-way ANOVA, Figs. 2a-2c) in response to amendments of the distinct bacterial preys. In most cases, growth rate and GGE parameters differed significantly for the same prey items utilized by different grazer type (Fig. 2). These parameters were generally higher in the axenic *Poterioochromonas* culture (e.g. the highest GGE values of 49, 47 and 44% detected in the II-D5, 2KL-1, and 2KL-27 treatments, respectively) compared to the mixed HNF community (Fig. 2b). Only the MoIso2 treatment, where smaller cells of the bacterial strain (MCV - 0.049 μm^3, Table 1) were fed to the relatively large flagellate *Poterioochromonas* sp. (cell diameter of 5-6 μm), showed an opposite trend, with significantly lower growth rate and GGE compared to the corresponding natural HNF community. Notably, the strain MWH-Wo1 (Luna 2 cluster, with larger cell volume than that of MoIso2, *see* Table 1), did not support any *Poterioochromonas* growth and also induced very limited growth of HNF with GGE values not exceeding 2.5% and lag phase longer than 70 h (Figs. 2a–2c). Compared to the growth rate and the GGE, the lag phase differed significantly only in one case (the strain II-B4) between the two grazer types.

Prey-specific differences in flagellate growth responses

To examine general trends in bacterial prey-specific growth responses across all experiments conducted with natural HNF communities from the Římov Reservoir and Lake Cep (*see* Table 2 for details), we first pooled all available triplicate data obtained from the same bacterial prey amendments independent of the season during which the experiments were conducted (Fig. 3). Note that some strains were used repeatedly during different plankton successional phases from April to October, reflected in large strain-specific variability in growth data (Fig. 3, e.g. the strain II-D5 used in seven triplicated experiments that yielded a sum of 21 treatments). Some other strains were used only in one particular

348 experiment with HNF (thus representing only one set of triplicate treatments, e.g. 2KL-1,
349 2KL-27; *see* Tables 1 and 2).
350 Though the boxplots shown in Figs. 3a,c,e indicated very large variability in HNF growth
351 parameters, these strain-specific data for growth rate, GGE and the length of lag phase
352 significantly differed (for details *see* Suppl. Information Table S2) among all bacterial strains
353 tested ($p < 0.001$, One-way ANOVA, followed by Tukey multiple comparison test). Thus for
354 instance, strain 2KL-27 supported significantly slower HNF growth rate ($p < 0.05$, Tukey test)
355 compared to other eleven strains from *Limnohabitans* and *Polynucleobacter* lineages. The
356 food characteristics of the strains 2KL-3 and of *M. turicensis* yielded significantly smaller
357 GGE ($p < 0.001$ and $p < 0.05$, respectively) compared to other seven strains. Interestingly,
358 significant differences ($p < 0.05$, Suppl. Information Table S2) were found even among
359 closely related strains from the Lim C lineage in growth rate (2KL-27 versus II-B4, II-D5,
360 Rim28, T6-5, 2KL-3 and Rim47) and GGE (e.g. 2KL-3 versus II-B4 and Rim28 strains,
361 Suppl. Information Table S2). However, prey amendments with the strain MWH-Wo1 (Luna 2
362 cluster) clearly yielded the most distinct HNF growth responses. They yielded frequently
363 significantly longer lag phase, in 8 cases they differed significantly in combination of two
364 parameters from other prey amendments (most frequently long lag phase coupled with low
365 GGE; Figs. 3b,c), or even in all three HNF growth parameters simultaneously (Suppl.
366 Information Table S2).
367 The data in Figs. 3a,c,e revealed typical range of values in net HNF maximum growth
368 rate, volumetric GGE and lag phase after prey amendments for each strain. For instance,
369 generally all strains, with the exception of the Luna 2 strain, supported relatively rapid growth
370 with considerably high GGE values. The mean and median values for all growth measures
371 detected for the strain MWH-Wo1 (Luna 2 in Figs. 3a,c,e) indicated a low nutritional value of
372 this prey for HNF communities. In most cases, these treatments yielded rather low growth

373 rate, GGE, and fairly long lag phase, reflecting a generally long adaptation period before the
374 HNF communities displayed any measurable growth.

375 Box plots in Figs. 3b,d,f present variability and mean and median values of the growth
376 parameters across all strains tested (a sum of 129 pooled treatments originating from 43
377 triplicate prey-amendment experiments). This gives estimates of growth of planktonic HNF
378 with mean and median growth rates of 1.61 d^{-1} and 1.66 d^{-1} (community doubling times of
379 10.3 and 10.1 h, respectively). For comparison, Fig. 3b shows also variability in growth rate
380 of HNF communities growing in planktonic samples from the Římov Reservoir filtered
381 through 5 μm-pore-size filters (removing HNF predators) and incubated in dialysis bags in
382 situ without any bacterial prey amendments (21 treatments taken from Šimek et al. 2006).
383 These treatments, where the growing HNF populations grazed only on indigenous
384 bacterioplankton supplied by nutrients coming from an ambient environment through a
385 dialysis membrane, yielded quite similar mean and median values of 1.75 d^{-1} and 1.59 d^{-1}
386 (corresponding to doubling times 9.5 and 10.5 h, respectively).

387 Most volumetric GGE values (5^{th}/95^{th} percentile) ranged between 16–38%, with very
388 small differences between the mean and median values (28.4% and 29.6%, respectively; Fig.
389 3d). However, some strains yielded either very high mean GGE values over 41% (strain Lim8
390 from the LimA lineage of the genus *Limnohabitans*), or very low mean GGE of < 12%
391 detected for the strain MWH-Wo1 from the Luna 2 cluster. Also the length of the lag phase
392 before the onset of HNF growth ranged considerably even for a given strain. Across all strains
393 tested most of the lag phase duration values (5^{th}/95^{th} percentile) ranged between 0.5–35 h,
394 with similar mean and median values (16.6 h and 16 h, respectively; Fig. 3f). The Luna 2
395 cluster (MWH-Wo1) strain was again an outlier, with the longest lag phase (Fig. 3e).

396 **Relationships between growth parameters of flagellates**

Regardless of the high variability in growth parameters (Figs. 1−3), some general trends were also obvious. High GGE values for particular treatments were usually accompanied by a short lag phase and relatively high values of maximum growth rate (*see* e.g. the strains II-D5 and 2KL-1 in *Poterioochromonas* treatments, Fig. 2). In contrast, the treatments amended with the Luna 2 cluster (MWH-Wo1) strain exemplify an opposite trend, with slow HNF growth or no growth (*Poterioochromonas* culture), in combination with low GGE values and fairly long lag phase (Figs. 2, 3a,c,e).

To confirm these trends statistically we used data from all experiments conducted with both predator types and plotted mean values (48 triplicate treatments; Fig. 4). The linear regression analysis indicated a highly significant inverse relationship between the length of the lag phase on one side, and the maximum growth rate and GGE on the other side (Figs. 4a,b). Approximately 22% and 59% of variability in maximum growth rate and GGE, respectively, were explained by the variability in the length of lag phase. In contrast, GGE values were significantly positively correlated with maximum growth (Fig. 4c).

Interestingly, very high volumetric GGE values were detected in the *Poterioochromonas* predator treatments (~40−49.6%, red symbols in Fig. 2b) amended by 4 strains from the LimC lineage of *Limnohabitans* that form a separate cluster in Fig. 4a. In contrast, 9 bacterial strains from this lineage used in 29 treatments with natural HNF communities (Table 2) did not show similarly high GGE values (Fig. 4a), yet the growth rates were comparable for both predator types (Fig. 4b). Generally, the results obtained with the strains from the LimC, LimB, and PnecC lineages, as well as for the Luna 2 cluster showed a rather broad variability in growth parameters (Figs. 3, 4). Moreover, the data for the Luna 2 strain suggested a low nutritional value of this prey for HNF except for one data point. Moreover, we detected no growth of *Poterioochromonas* on this strain even after 112 h of the experiment (data not shown). Thus this “zero growth” point could not be used in the regression analysis while it clearly indicated

422 inappropriateness of the prey for the predator. In contrast, in all other cases we detected
423 measurable flagellate growth already within 66 h of the experiment, as shown in Figs. 4a,b.

424 **Lineage- and season-specific differences in HNF growth responses to prey amendments**

425 For further testing we selected only treatments where the same strain or strains affiliated
426 to the same bacterial lineage were used in at least 2 seasonally different experiments in Římov
427 Reservoir or Lake Cep. Thus, four lineage-specific data sets were assembled (Suppl.
428 Information Fig. S9): (i) Luna 2, the strain MWH-Wo1 was used in four experiments; (ii)
429 LimB, strain Rim11 was used in four experiments; (iii) LimC, nine distinct strains were used,
430 some of them tested repeatedly in ten experiments; and (iv) PnecC, two strains used in two
431 experiments (*see* Table 2). The differences in HNF prey-specific growth responses were first
432 tested among these 4 prey groups independent of the season. The data characterizing growth
433 responses of HNF to the strain from the Luna 2 cluster significantly differed in all growth
434 parameters from the other three bacterial prey categories ($p < 0.05$, Suppl. Information Fig.
435 S9). In contrast, we did not find significant differences ($p > 0.05$) in HNF growth responses to
436 prey amendments with strains from LimB, LimC, and PnecC prey categories.

437 To reveal season-specific aspects of growth responses of HNF communities to the 4
438 bacterial prey categories defined previously (*see* Suppl. Information Fig. S9) we tested
439 separately the data from experiments conducted in April, May, August, and October (Fig. 5,
440 Suppl. Information Table S1). Independent of the season the data for the Luna 2 cluster strain
441 always differed significantly (two-way ANOVA, $p < 0.05$) in the growth parameters from
442 other three bacterial prey categories. However, overall variability in HNF growth rate (Figure
443 5a−d), as a response to amendments with the four prey categories, did not differ significantly
444 over the four seasonal phases ($p > 0.05$). Significant season-specific differences ($p < 0.05$)
445 were detected for GGE values in May (rather low values, Fig. 5f) and August (generally high
446 GGE, Fig. 5g) that both differed from April and October data (Figs. 5e,h). However, the latter

two data sets for GGE did not significantly differ one from another. The shortest lag phase (below 2.6 h) and significantly higher GGE values were detected for August compared to other seasons. Overall, the combination of growth parameters detected in August treatments, i.e. the highest GGE and shortest lag phase (Figs. 5g,k), indicated the minimum time needed for the indigenous HNF communities to adapt to particular prey amendments (Table 2, Suppl. Information Figs. S5 and S7).

We also tested season-specific differences in median cell volume of HNF (Suppl. Information Fig. S10). Only in the May samples (clear water phase) the flagellate cells were significantly smaller (median 10.5 μm^3, $p < 0.001$) compared to other phases with median values around 20 μm^3. Notably, in samples used in experiments done in May, also the median and mean values of HNF cell volume were almost identical, thus indicating a rather uniform small cell size of HNF. This fact was partially reflected in the combination of generally longer lag phase and lower GGE values in May, when the small flagellate cells were suddenly exposed to generally large bacteria from LimC lineage, such as the strains T6-5 and 2KL-1 (Tables 1 and 2). Interestingly, however, only in late May (experiment XI, Table 2) the offered smaller cells of the Luna 2 strain (Table 1) induced more rapid HNF growth (Figs 5b,f,j).

Discussion

Major findings

We examined the growth potential and biomass transfer efficiency of natural HNF communities feeding on a very broad spectrum of relevant planktonic bacterial groups so far not employed in previous investigations (cf. Šimek et al. 2013; Grujčić et al. 2015; Weisse et al. 2016). Moreover, our study has brought new insights into food quality aspects of the prey bacteria and revealed both general and prey-specific trends in the growth responses of natural HNF communities to changing prey food quality represented by 16 distinct bacterial strains (Figs. 1–4). We found many significant differences in the responses of HNF communities to

the prey amendments by distinct, but also by closely related bacterial strains (Suppl. Information Table S2). Moreover, we demonstrated that even the same bacterial prey can produce different HNF growth responses depending upon the season (Fig. 5), being likely related to marked compositional shifts in temporally evolving flagellate grazer communities (Domaizon et al. 2003; Mangot et al. 2013).

Effects of prey food quality on flagellate growth

Our results document a large variability in HNF growth responses (Figs. 3, 4) with many season-specific aspects (Fig. 5) related to different temporal community dynamics of bacterivorous HNF that have been previously described (e.g., Šimek et al. 1997; Domaizon et al. 2003; Nolte et al. 2010). However, the responses of the natural grazer communities to enrichment with particular prey over different plankton successional phases have rarely been demonstrated (Grujčić et al. 2015). Additionally, comparisons of the same prey amendments in samples from the reservoir and the lake revealed significant differences in HNF growth parameters that can be related to different seasonal succession of plankton and different trophic status of the lakes (experiments III–VI, for a detailed analysis *see* also Grujčić et al. 2015). Thus, e.g. prey amendment with relatively large bacterial cells, such as those of the 2KL-3 strain (Table 1), can paradoxically support rather low growth rate and GGE values during clear water phase with small flagellate cell sizes present (cf. Suppl. Information Fig. S10), likely due to a shift to suboptimal predator-prey size ratio (Hansen et al. 1994; Boenigk et al. 2004). It can even significantly reduce the transfer efficiency from such a prey (Fig. 3, Suppl. Information Table S2) and so also the significance of the bacteria-HNF trophic link.

To our knowledge none of the strains used in this study displayed any detectable morphology-related traits of grazing-resistance such as flock- or filament-formation (Hahn and Höfle 2001; Jürgens and Matz 2002). Moreover, using group-specific FISH-probes all bacterial prey types were observed in flagellate food vacuoles, as exemplified in Šimek et al.

2013 (Suppl. Fig. 1 therein) and Grujčić et al. 2015 (Fig. 4 therein). In all cases, we also observed a prey abundance decrease during the course of the experiments (*see* examples in Fig. 1). This holds even true for the gram-positive MWH-Wo1 strain (Luna 2 cluster), which supported no (*Poterioochromonas*) or frequently only very limited growth of flagellate predators (Figs. 2,3). However, in one experiment only (XI, Table 2) this apparently less utilizable prey (MWH-Wo1 strain, *see* also Tarao et al. 2009) of medium cell size (Table 1) supported considerably elevated HNF growth rate with GGE of ~ 19% (Figs. 5b,f), which clearly points to the significance of the initial composition of the grazer community used in the experiment. We anticipate that natural HNF assemblages contain also bacterivorous flagellates that can relatively efficiently utilize gram-positive *Actinobacteria* considered to be partially grazing-protected (Pernthaler et al. 2001). Members of the Luna 2 cluster are assumed to be grazing resistant due to specific surface structures of their cell walls (Tarao et al. 2009). Notably, all strains were likely at least partially utilizable by the flagellates, although the different prey food quality results in the large prey-specific variability in HNF growth parameters (Figs. 3-5, Suppl. Information Table S2). An intriguing question then arises: how much time does it takes before the HNF community composition shifts to efficiently utilize the available bacterial prey? Notably, many strains supported relatively rapid growth and hence the differences in lag phase seem to be related to the "adaptation time" needed to optimize the grazer community composition to perform well on the available bacterial prey (Šimek et al. 2013).

The culture of *Poterioochromonas* showed mostly significantly higher GGE values when growing on strains from the LimC lineage of *Limnohabitans* compared to the HNF community growing on the same prey items (Fig. 2a). However, even the high GGE values of 39–49% are well within the range of data obtained in laboratory experiments with various protistan cultures (Straile 1997). Thus the food quality of the LimC strains and their suitable

522 cell sizes (Table 1) were likely the primary reasons yielding the high GGE values obtained
523 with the predator culture (experiment IB). In contrast, the smaller cell size of the bacterial
524 strain MoIso2 (PnecD lineage, Table 1) and its specific food quality aspects compared to the
525 strains from Lim C lineage (used in both experiments IA and IB, Table 2) likely limited the
526 growth of this flagellate culture. However, the natural HNF community, composed of a mixed
527 community of flagellate grazers of various sizes, grew on the strain MoIso2 at rates
528 comparable to those achieved by HNF growing on the strains from the LimC lineage of
529 *Limnohabitans* (experiment IA, Fig. 2).

530 **Estimates of HNF growth rate and growth efficiency**

531 The prey-amended natural HNF communities yielded mean community doubling time of
532 10 h and volumetric GGE around 29% (Figs. 3b,d). Also some previous studies (Jürgens and
533 Matz 2002; Weisse et al. 2016 and references therein) reported very rapid doubling times of
534 HNF communities in situ, comparable to our growth results (Fig. 3b). Moreover, our GGE
535 estimates fit quite well the literature values of GGE reviewed in Straile (1997), based on
536 numerous studies dealing with growth efficiency of both macro- and microzooplankton
537 groups including laboratory cultures of small protists.

538 Notably, in situ studies where no bacterial prey was added into < 5 μm treatments
539 (removal of zooplankton predators of HNF) and samples were incubated in dialysis bags in
540 the Římov Reservoir (Jezbera et al. 2006; Šimek et al. 2006), showed a relatively similar
541 range of HNF growth rates (Fig. 3b). In fact, these dialysis bag incubations in the reservoir
542 can be considered as a measure of "carrying capacity" of this plankton environment in terms
543 of the carbon pool available for growth of indigenous bacteria that fueled the HNF community
544 growth in temperatures of 13−24^{o}C (Šimek et al. 2006). In both types of experimental
545 incubations, the HNF maximum growth rates and abundance peaks were mostly achieved in
546 36–72 h (compare examples of HNF growth curves in Suppl. Information Figs. S1–S8). Thus

547 our experimental prey amendments mimicked quite well, at least in terms of organic carbon
548 introduced in bacterial biomass (I–XI, Table 2), the amount and rates of biomass transfer from
549 bacteria to HNF in the reservoir plankton.

550 Theoretically one should assume faster growth potential of prey bacterial communities
551 because they are dominated by cells with approximately two orders of magnitude smaller cell
552 volumes compared to their flagellate grazers (Hansen et al. 1994; Boukal 2014). However,
553 since bacteria are at the bottom of the food chain of a complex pelagic environment they are
554 likely to be more strongly bottom-up than top-down controlled (McQueen et al. 1986; Gasol
555 and Vaqué 1993), apart from being selectively top-down controlled by protistan grazing and
556 viruses (Jürgens and Matz 2002; Weinbauer 2004). Thus it is not surprising that the same
557 bacterial phylotypes (targeted by FISH probes) grow more slowly in situ than representative
558 bacterial isolates from the same taxon do grow in substrate-optimized pure culture conditions
559 (Kasalický et al. 2013). In contrast, small bacterivorous flagellates in our meso- and eutrophic
560 study systems, with bacterial densities of 1.5–4.5 × 10^6 cells ml^{-1} (Table 2), were likely close
561 to the saturation prey levels and thus HNF grew very rapidly, close to their maximum growth
562 rates (Jürgens 1992; Arndt et al. 2000). However, HNF are usually top-down regulated by
563 micro- and macrozooplankton (Jürgens et al. 1996; Zöllner et al. 2003; Šimek et al. 2014),
564 which can explain the lack of a simple coupling between the abundance of bacterivorous HNF
565 and their bacterial prey in some pelagic systems (Gasol and Vaqué 1993).

566 **Rapid shifts in interacting flagellate predator-bacterial prey communities**

567 Our estimates of HNF growth rates (Fig. 3) resemble tightly the maximum growth rates
568 detected in rapidly growing bacterioplankton groups considered as “algal bloom specialists”,
569 such as those of *Limnohabitans*, *Fluviicola* sp. and species-like tribes of *Flavobacteria* (Zeder
570 et al. 2009; Eckert et al. 2012; Neuenschwander et al. 2015). Their short-lived peaks, co-
571 occurring with various phytoplankton taxa, last usually for a few days only and are frequently

572 terminated by enhanced HNF abundance and bacterivory (Zeder et al. 2009; Eckert et al.
573 2012; Šimek et al. 2014). The latter studies, based on the use of specific FISH-probes,
574 indicated that abundances of rapidly growing bacterial taxa double within 6 to 20 hours.
575 Thus importantly, the major taxa of bacterioplankton prey (e.g. Zeder et al. 2009; Eckert
576 et al. 2012) as well as predator communities (Arndt et al. 2000; Boenigk and Arndt 2002;
577 Jürgens and Matz 2002) possess high growth potential that apparently contributes to their
578 relative growth balance in situ as suggested in a simplified conceptual model (Fig. 6).
579 However, a broad array of major bottom-up and top-down controlling factors, such as shifts in
580 resource availability or in major bacterial mortality factors (Fig. 6a), can either accelerate or
581 slow down the growth of both prey and predator populations (Gasol and Vaqué 1993). Rapid
582 shifts in major top-down and bottom-up regulating factors can either result in temporal growth
583 imbalance (phases 2 and 4 in Fig. 6b) in the predator-prey assemblages, or re-establishment of
584 the growth balance but already at different, either low or high rates (Fig. 6b, *see* phases 1 and
585 3, respectively). Then, for instance, a sudden pulse in nutrient availability can induce the
586 outgrowth of rapidly dividing bacterial species (predicted by phase 2 in Fig. 6b) that would
587 then result in species-specific short-lived peaks of particular bacterial species (Zeder et al.
588 2009; Eckert et al. 2012; Šimek et al. 2014). Such an environmental scenario (observed
589 mainly during spring bloom phases, e.g. Šimek et al. 2014 and references therein), diverts the
590 predator-prey system to temporal growth imbalance with higher bacterial cell production than
591 bacterial loss rates (Gasol and Vaqué 1993) till more abundant, or rapidly growing and likely
592 distinct flagellate predator groups appear (phase 3, Fig. 6b). Such rapid flagellate community
593 shifts induced by changing prey food quality and availability have already been demonstrated
594 in the experiment IA (Šimek et al. 2013) and experiment X (V. Grujčić and K. Šimek, unpubl.;
595 *see* also the text below).

596 We are aware that the proposed model oversimplifies the complexity of this trophic
597 linkage and thus cannot reflect all naturally occurring predator-prey interactions. However, we
598 hypothesize that major driving forces that fine tune these trophic interactions are not just
599 changes in abundance, but mainly marked community shifts at both prey (Jürgens and Matz
600 2002; Šimek et al. 2006) and predator levels (Šimek et al. 2013), as proposed in our model
601 (Fig. 6b). The rapid and significant community shifts optimize survival strategies and growth
602 responses at both trophic levels. Disturbances at either side of the trophic link ((due to e.g.
603 resource depletion for bacteria (Gasol and Vaqué 1993), or enhanced zooplankton predation
604 on flagellates (Jürgens et al. 1996)) induce marked responses that facilitate temporal re-
605 establishment of the relative growth balance at different growth rates, however, already with
606 differentially composed predator prey communities (Figs. 6a,b).
607 The model predictions are supported by evidence from both field and laboratory studies.
608 For instance, specific analyses of flagellate food vacuole contents clearly demonstrated both
609 positive selections for, and negative selection against, certain bacterial taxa in plankton
610 samples (Jezbera et al. 2006; Šimek et al. 2014). Feedbacks of bacterial food quality on
611 predator community composition and growth are important but unfortunately rarely studied
612 (Weisse et al. 2016). Notably, sequence data demonstrated that significant prey-specific shifts
613 in the HNF predator communities were induced by sudden shifts in bacterial prey availability
614 (experiment IA, for details *see* Šimek et al. 2013). Moreover, in the light of our data, we
615 assume that these shifts can be strongly season-specific (Fig. 5). For instance, we used closely
616 related *Limnohabitans* strains from the LimC lineage in two experiments with samples from
617 the Římov Reservoir, scheduled during different seasons (IA and X, Table 2). In the spring
618 experiment IA (April 2011), an analysis of eukaryotic 18S rDNA sequences showed strong
619 prey-specific HNF community shifts within *Stramenopiles*, being reflected at higher
620 taxonomic resolution mainly through changing proportions of bacterivorous chrysophytes –

621 i.e., *Pedospumella* and several *Spumella*-related lineages (for details *see* Šimek et al. 2013). In
622 the summer experiment X (August 2014, Table 2), 18S rDNA sequencing and quantification
623 of some major groups of bacterivorous flagellates by specific FISH probes resulted in a
624 different initial HNF community, dominated by colorless members of the phagotrophic
625 *Cryptophyta*, its CRY1 lineage (Piwosz et al. 2016) or phagotrophic *Katablepharidophyta* (V.
626 Grujčić, unpubl.). Notably, prey-specific HNF community shifts in this experiment were
627 mediated mainly through changing proportions of bacterivorous lineages of *Cryptophyta* and
628 *Choanoflagellida* (V. Grujčić, unpubl.). This comparison illustrates that even closely related
629 prey items can induce temporarily quite different patterns of prey-specific HNF community
630 shifts; a phenomenon that has rarely been documented so far.
631 The shifts in both prey and predator communities are likely closely interconnected and
632 occur within a time span of approximately half a day to a few days. The shifts in flagellate
633 communities may be the result of rarer taxa becoming dominant with changing environmental
634 conditions (Caron and Countway 2009; Nolte et al. 2010). In this study, we demonstrated that
635 such rapid adaptations of the predator community have fundamental importance for the
636 efficiency of organic matter transfer to the grazer food chain. The rapid HNF community
637 shifts (Fig. 6b) and flagellate selective feeding on fast-growing or larger bacteria (thus
638 cropping bacterial production rather than the standing stocks, Sherr and Sherr 2002; Jezbera et
639 al. 2005) are changing our views on time scales at which substantial changes in carbon flow
640 can occur. However, to document these processes at high taxonomic resolution in situ, there is
641 an urgent need to establish novel detection techniques, such as CARD-FISH with highly
642 specific probes (Massana et al. 2009; Piwosz and Pernthaler 2010 Mangot et al. 2013) that
643 would allow us to precisely quantify major freshwater flagellate bacterivores without sample
644 manipulation.
645

References

Arndt, H., D., Dietrich, B., Auere, E.-J., Cleven, T., Gräfenhan, M., Weitere, and A.P. Mylnikov. 2000. Functional diversity of heterotrophic flagellates in aquatic ecosystems, p. 240–268. In B. S. C. Leadbeater and J. C. Green [eds.], The Flagellates. London, UK: Taylor and Francis.

Boenigk, J., and H. Arndt. 2002. Bacterivory by heterotrophic flagellates: community structure and feeding strategies. Anton. Leeuw. Int. J. G. **81:** 465–480.

Boenigk, J., K., Pfandl, and P. J. Hansen. 2006. Exploring strategies for nanoflagellates living in a 'wet desert'. Aquat. Microb. Ecol. **44:** 71–83.

Boenigk, J., P. Stadler, A. Wiedlroither and M. W. Hahn. 2004. Strain-specific differences in the grazing sensitivities of closely related ultramicrobacteria affiliated with the *Polynucleobacter* cluster. Appl. Environ. Microbiol. **70**: 5787–5793.

Boukal, D. S. 2014. Trait- and size-based descriptions of trophic links in freshwater food webs: current status and perspectives. J. Limnol. **73:** 171–185.

Caron, D.A., and P. D. Countway. 2009. Hypotheses on the role of the protistan rare biosphere in a changing world. Aquat. Microb. Ecol. **57:** 227–238.

Chrzanowski, T. H., and B. L. L. Foster. 2014: Prey element stoichiometry controls ecological fitness of the flagellate *Ochromonas danica*. Aquat. Microb. Ecol. **71:** 257–269.

Corno, G., J. Villiger, and J. Pernthaler. 2013. Coaggregation in a microbial predator-prey system affects competition and trophic transfer efficiency. Ecology **94:** 870–81.

Domaizon, I., S. Viboud, and D. Fontvieille . 2003. Taxon-specific and seasonal variations in flagellates grazing on heterotrophic bacteria in the oligotrophic Lake Annecy - importance of mixotrophy. FEMS Microbiol. Ecol. **46:** 317–329.

669 Eckert, E. M., M. Baumgartner, I. M. Huber, and J. Pernthaler. 2013. Grazing resistant
670 freshwater bacteria profit from chitin and cell-wall-derived organic carbon. Environ.
671 Microbiol. **15:** 2019–2030.
672 Eckert, E. M., M. M., Salcher, T. Posch, B. Eugster, and J. Pernthaler. 2012. Rapid
673 successions affect microbial N-acetyl-glucosamine uptake patterns during a lacustrine
674 spring phytoplankton bloom. Environ. Microbiol. **14:** 794–806.
675 Eiler, A., and S. Bertilsson. 2007. Flavobacteria blooms in four eutrophic lakes: Linking
676 population dynamics of freshwater bacterioplankton to resource availability. Appl.
677 Environ. Microbiol. **73:** 3511–3518.
678 Gasol, J.M., and P. A. del Giorgio. 2000. Using flow cytometry for counting natural
679 planktonic bacteria and understanding the structure of planktonic bacterial
680 communities. Sci. Mar. **64:** 197–224.
681 Gasol, J. M., and D. Vaqué. 1993. Lack of coupling between heterotrophic nanoflagellates and
682 bacteria: A general phenomenon across aquatic systems? Limnol. Oceanogr. **38:** 657–665.
683 Grujčić, V., V. Kasalický, and K. Šimek. 2015. Prey-specific growth responses of freshwater
684 flagellate communities induced by morphologically distinct bacteria from the genus
685 *Limnohabitans.* Appl. Environ. Microbiol. **81:** 4993–5002.
686 Hahn, M. W, and M. G. Höfle. 2001. Grazing of protozoa and its effect on populations of
687 aquatic bacteria. FEMS Microbiol. Ecol **35:** 113–121.
688 Hahn, M. W., E. Lang, U. Brandt, H. Lünsdorf, Q. L. Wu, and E. Stackebrandt. 2010.
689 *Polynucleobacter cosmopolitanus* sp. nov., free-living planktonic bacteria inhabiting
690 freshwater lakes and rivers. Int. J. Syst. Evol. Microbiol. **60:** 166–173.
691 Hahn, M. W., E. R. B. Moore, and M. G. Höfle. 1999. Bacterial filament formation, a defense
692 mechanism against flagellate grazing, is growth rate controlled in bacteria of different
693 phyla. Appl. Environ. Microbiol. **65:** 25–35.

694 Hahn, M. W., and M. Pöckl. 2005. Ecotypes of planktonic *Actinobacteria* with identical 16S
695 rRNA genes adapted to thermal niches in temperate, subtropical, and tropical freshwater
696 habitats. Appl. Environ. Microbiol. **71:** 766−773.
697 Hahn, M. W., M. Pöckl, and Q. L. Wu. 2005. Low intraspecific diversity in a
698 *Polynucleobacter* subcluster population numerically dominating bacterioplankton of a
699 freshwater pond. Appl. Environ. Microbiol. **71:** 4539–4547.
700 Hahn, M. W., P. Stadler, Q. L. Wu, and M. Pöckl 2004. The filtration acclimatization method
701 for isolation of an important fraction of the not readily cultivable bacteria. J. Microbiol.
702 Methods **57:** 379–390.
703 Hansen, B., P. K. Bjornsen and P. J. Hansen 1994. The size ratio between planktonic predators
704 and their prey. Limnol. Oceanogr. **39:** 395−403.
705 Jezbera, J., K. Horňák, and K. Šimek. 2005. Food selection by bacterivorous protists: insight
706 from the analysis of the food vacuole content by means of fluorescence in situ
707 hybridization. FEMS Microbiol. Ecol. **52:** 351−363.
708 Jezbera, J., K. Horňák, and K. Šimek. 2006. Prey selectivity of bacterivorous protists in
709 different size fractions of reservoir water amended with nutrients. Environ. Microbiol. **8:**
710 1330−1339.
711 Jezbera, J.**,** J. Jezberová, U**.** Brandt, and M.W. Hahn. 2011. Ubiquity of *Polynucleobacter*
712 *necessarius* subspecies *asymbioticus* results from ecological diversification. Environ.
713 Microbiol. **13**: 922–931.
714 Jezbera, J.**,** J. Jezberová, U. Koll, K. Horňák, K. Šimek, and M. W. Hahn. 2012. Contrasting
715 trends in distribution of four major planktonic *Betaproteobacteria* groups along a pH
716 gradient of epilimnia of 72 freshwater habitats. FEMS Microbiol. Ecol. **81:** 467–479.
717 Jezberová J., J. Jezbera, P. Znachor, J. Nedoma, V. Kasalický, and K. Šimek. 2017:
718 *Limnohabitans* genus harbor generalist and opportunist genotype groups: evidence from

719 spatiotemporal succession in a canyon-shaped reservoir. Appl. Environ. Microbiol. 83
720 (21); in press, DOI:10.1128/AEM.01530-17

721 Jürgens, K. 1992. Is there plenty of food for bacterivorous flagellates in eutrophic waters?
722 Arch. Hydrobiol. Beih. Ergebn. Limnol. **37:** 195–205.

723 Jürgens, K., and C. Matz. 2002. Predation as a shaping force for the phenotypic and genotypic
724 composition of planktonic bacteria. Anton. Leeuw. Int. J. G. **81:** 413–434.

725 Jürgens, K., S. A. Wickham, K. O. Rothhaupt, and B. Santer. 1996. Feeding rates of macro-
726 and microzooplankton on heterotrophic nanoflagellates. Limnol. Oceanogr. **41:** 1833–
727 1839.

728 Kasalický, V., J. Jezbera, K. Šimek, and M. W. Hahn. 2010. *Limnohabitans planktonicus* sp.
729 nov., and *Limnohabitans parvus* sp. nov., two novel planktonic *Betaproteobacteria*
730 isolated from a freshwater reservoir. Int. J. Syst. Evol. Microbiol. **60:** 2710–2714.

731 Kasalický, V., J. Jezbera, M. W. Hahn, and K. Šimek. 2013. The diversity of the
732 *Limnohabitans* genus, an important group of freshwater bacterioplankton, by
733 characterization of 35 isolated strains. PLOS ONE **8:** e58209.

734 Kopáček, J., and J. Hejzlar. 1993. Semi-micro determination of total phosphorus in fresh
735 waters with perchloric acid digestion. Int. J. Environ. Anal. Chem. **53:**173–183.

736 Lorenzen, C. J. 1966. Determination of chlorophyll and phaeopigments: spectrophotometric
737 equation. Limnol. Oceanogr. **12:** 343–346.

738 Mangot, J.-F., I. Domaizon, N. Taib, N. Marouni, E. Duffaud, G. Bronner, and D. Debroas
739 2013. Short-term dynamics of diversity patterns: evidence of continual reassembly within
740 lacustrine small eukaryotes. Environ. Microbiol. **15**: 1745–1758.

741 Massana, R., F. Unrein, R. Rodríguez-Martínez, I. Forn, T. Lefort, J. Pinhassi, and F. Not.
742 2009. Grazing rates and functional diversity of uncultured heterotrophic flagellates. ISME
743 J. **3:** 588–596.

744 McQueen, D. J., J. R. Post, and E. L. Mills. 1986. Trophic relationships in freshwater pelagic
745 ecosystems. Can. J. Fish. Aquat. Sci. **43:** 1571–1581.
746 Montagnes, D. J. S., and others. 2008: Selective feeding behaviour of key free-living protists:
747 avenues for continued study. Aquat. Microb. Ecol. **53:** 83–98.
748 Murphy, J., and J. Riley. 1962. A modified single solution method for the determination of
749 phosphate in natural waters. Anal. Chim. Acta **27:**31–36.
750 Nakano, S., P. M. Manage, Y. Nishibe, and Z Kawabata. 2001. Trophic linkage among
751 heterotrophic nanoflagellates, ciliates and metazoan zooplankton in a hypereutrophic
752 pond. Aquat. Microb. Ecol. **25:** 259–270.
753 Neuenschwander, S. M., J. Pernthaler, T. Posch, and M. M. Salcher. 2015. Seasonal growth
754 potential of rare lake water bacteria suggests their disproportional contribution to carbon
755 fluxes. Environ. Microbiol. **17:** 781−795.
756 Newton, R. J., S. E. Jones, A. Eiler, K. D. McMahon, and S. Bertilsson. 2011. A guide to the
757 natural history of freshwater lake bacteria. Microbiol. Mol. Biol. Rev. **75:** 14−49.
758 Nolte, V., R. V. Pandey, S. Jost, R. Medinger, B. Ottenwälder, J. Boenigk, and C.
759 Schlöttenrer. 2010. Contrasting seasonal niche separation between rare and abundant taxa
760 conceals the extent of protist diversity. Mol. Ecol. **19:** 2908–2915.
761 Pernthaler, A., J. Pernthaler, and R. Amann. 2002. Fluorescence in situ hybridization and
762 catalyzed reporter deposition for the identification of marine bacteria. Appl. Environ.
763 Microbiol. **68:** 3094–3101.
764 Pernthaler, J., T. Posch, K. Šimek, J. Vrba, U. Nübel, F.-O. Glöckner, R. Psenner, and R.
765 Amann. 2001: Predator-specific enrichment of *Actinobacteria* from a cosmopolitan
766 freshwater clade in a mixed continuous culture. Appl. Environ. Microbiol. **67:** 2145–2155.
767 Piwosz, K, J. Kownacka, A. Ameryk, M. Zalewski, and J. Pernthaler. 2016. Phenology of
768 cryptomonads and the CRY1 lineage in a coastal brackish lagoon (Vistula Lagoon, Baltic

769 Sea). J. Phycol. **52:** 626–637.
770 Piwosz, K., and J. Pernthaler. 2010. Seasonal population dynamics and trophic role of
771 planktonic nanoflagellates in coastal surface waters of the Southern Baltic Sea. Environ.
772 Microbiol. **12:** 364–377.
773 Salcher, M. M. 2014. Same same but different: ecological niche partitioning of planktonic
774 freshwater prokaryotes. J. Limnol. **73:** 74−87.
775 Salcher, M. M., S. M. Neuenschwander, T. Posch, and J. Pernthaler. 2015. The ecology of
776 pelagic freshwater methylotrophs assessed by a high-resolution monitoring and isolation
777 campaign. ISME J. **9:** 2442–2453.
778 Salcher, M. M., J. Pernthaler, N. Frater, and T. Posch. 2011. Vertical and longitudinal
779 distribution patterns of different bacterioplankton populations in a canyon-shaped, deep
780 prealpine lake. Limnol.Oceanogr. **56:** 2027−2039.
781 Salcher, M. M., T. Posch, and J. Pernthaler. 2013. *In situ* substrate preferences of abundant
782 bacterioplankton populations in a prealpine freshwater lake. ISME J. **7:** 896−907.
783 Shabarova, T., V. Kasalický, K. Šimek, J. Nedoma, P. Znachor, T. Posch, J. Pernthaler, and M.
784 M. Salcher. 2017. Distribution and ecological preferences of the freshwater lineage LimA
785 (genus *Limnohabitans*) revealed by a new double hybridization approach. Environ.
786 Microbiol. **19:** 1296–1309.
787 Sherr, E. B., and B. F. Sherr. 2002. Significance of predation by protists in aquatic microbial
788 food webs. Anton. Leeuw. Int. J. G. **81:** 293–308.
789 Šimek, K., P. Hartman, J. Nedoma, J. Pernthaler, J. Vrba, D. Springmann, and R. Psenner.
790 1997: Community structure, picoplankton grazing and zooplankton control of
791 heterotrophic nanoflagellates in a eutrophic reservoir during the summer phytoplankton
792 maximum. Aquat. Microb. Ecol. **12:** 49–63.

793 Šimek, K., and others. 2006: Maximum growth rates and possible life strategies of different
794 bacterioplankton groups in relation to phosphorus availability in a freshwater reservoir.
795 Environ. Microbiol. **8:** 1613–1624.
796 Šimek, K., K. Horňák, J. Jezbera, J. Nedoma, P. Znachor, J. Hejzlar, and J. Seďa. 2008.
797 Spatio-temporal patterns of bacterioplankton production and community composition
798 related to phytoplankton composition and protistan bacterivory in a dam reservoir. Aquat.
799 Microb. Ecol. **51**: 249–262.
800 Šimek, K., and others. 2013. Differential freshwater flagellate community response to
801 bacterial food quality with a focus on *Limnohabitans* bacteria. ISME J. **7:** 1519–1530.
802 Šimek, K., J. Nedoma, P. Znachor, V. Kasalický, J. Jezbera, K. Horňák, and J. Seďa. 2014. A
803 finely tuned symphony of factors modulates the microbial food web of a freshwater
804 reservoir in spring. Limnol. Oceanogr. **59:** 1477–1492.
805 Šimek, K., J. Pernthaler, M. G. Weinbauer, K. Horňák, J. R. Dolan, J. Nedoma, M. Mašin,
806 and R. Amann. 2001. Changes in bacterial community composition, dynamics and viral
807 mortality rates associated with enhanced flagellate grazing in a meso-eutrophic reservoir.
808 Appl. Environ. Microbiol. **67:** 2723–2733.
809 Straile, D. 1997. Gross growth efficiencies of protozoan and metazoan zooplankton and their
810 dependence on food concentration, predator-prey weight ratio, and taxonomic group.
811 Limnol. Oceanogr. **42:** 1375–l385.
812 Tarao, M., J. Jezbera, and M. W. Hahn. 2009. Involvement of cell surface structures in size-
813 independent grazing resistance of freshwater *Actinobacteria*. Appl. Environ. Microbiol.
814 **75:** 4720–4726.
815 Weinbauer, M. 2004. Ecology of prokaryotic viruses. FEMS Microbiol. Rev. **28:** 127–181.
816 Weisse T., R. Anderson, H. Arndt, A. Calbet, P. J. Hansen, and D.J.S. Montagnes. 2016.
817 Functional ecology of aquatic phagotrophic protists – concepts, limitations, and

perspectives. Eur. J. Protistol. **55:** 50–74.

Zeder, M., S. Peter, T. Shabarova, and J. Pernthaler. 2009. A small population of planktonic *Flavobacteria* with disproportionally high growth during the spring phytoplankton bloom in a prealpine lake. Environ. Microbiol. **11:** 2676−2686.

Zöllner, E., B. Santer, M. Boersma, H. G. Hoppe, and K. Jürgens. 2003. Cascading predation effects of *Daphnia* and copepods on microbial food web components. Freshw. Biol. **48:** 2174–2193.

825 ***Acknowledgments***

826 We thank J. Hejzlar for chemical data analysis and J. Dolan for comments and English text
827 corrections. We also thank R. Ghai and D. Sirová for their valuable comments to the earlier
828 version of the manuscript; and H. Kratochvílová, R. Malá, and M. Štojdlová for their
829 excellent laboratory assistance. This study was largely supported by the Czech Science
830 Foundation under the research grant 13-00243S awarded to K.S. Additional support provided
831 the PhD student grant of the Faculty of Science (V.G.), University of South Bohemia (GAJU
832 04-145/2013/P).

Text to figures

Figure 1. Examples of time course changes in abundance (**a, c, e, g, i**) and biovolume of the mixotrophic bacterivorous flagellate *Poterioochromonas* sp. in comparison to bacterial biovolume (**b, d, f, h, j**) in the treatments amended with respective bacterial strains in experiment IB (further details *see* in Tables 1 and 2). The arrows in panel **b** highlight the data points selected to calculate volumetric GGE values. Full symbols in panels **a, c, e, g,** and **i** highlight the time points selected to calculate the maximum flagellate growth rate (slope = μ, *see* the arrow in panel **a**). The length of lag phase was calculated as the period from the time zero to the intercept between the best-fit line of the flagellate growth and the zero-time level of its abundance as depicted in panel **i**. Values are means of triplicates; error bars show SD. Data for the strain MWH-Wo1 and control treatments are not shown as no flagellate growth was detected.

Figure 2. Growth parameters of HNF communities versus *Poterioochromonas* sp. Maximum growth rate (**a**), gross growth efficiency (GGE, **b**), and length of lag phase after the treatment amendment (**c**) of a natural planktonic HNF community (Římov reservoir) in comparison to a culture of the bacterivorous flagellate *Poterioochromonas* sp. amended by additions of the same biovolume of different bacterial prey. The prey bacteria were 4 strains of the genus *Limnohabitans*, i.e., *L. planktonicus* (II-D5)*, L. parvus* (II-B4), 2KL-27 and 2KL-1, and the strains MoIso2 and Luna 2 (the MWH-Wo1 strain, for details *see* Tables 1 and 2). Values are means for triplicates; error bars show SDs. Different capital letters indicate a significant difference ($p < 0.05$, two-way ANOVA, followed by Unequal N HSD multiple comparison post-hoc test) between treatments amended with different bacterial strains. Stars above bars denote significant difference in the growth responses of the HNF community versus *Poterioochromonas* sp. growing on the same prey item. n.d. – no growth of *Poterioochromonas* on Wo1 was detected.

Figure 3. Overall variability in bacterial prey-specific responses across all experiments conducted with natural HNF communities from Římov reservoir and Cep Lake amended by additions of different bacterial strains. A total of 16 different bacterial strains were tested as HNF food, with some of them being used repeatedly during different plankton phases from April to October (for details *see* Table 1 and Fig. 5). Data variability of triplicate treatments in HNF maximum growth rate (**a**), volumetric GGE (**c**), and lag phase (**e**) are shown in box plots

with 5^{th}/95^{th} percentile (full symbols are outliers, full and dashed lines, median and mean value, respectively). The box plots representing the data for bacterial strains labeled by the strain codes (Table 1), situated to the left of the vertical dashed line in panels **a, c** and **e**, are affiliated to the LimC lineage of the genus *Limnohabitans*. Other six prey categories plotted right side of the dashed line belong to different bacterial lineages and are largely represented by only one bacterial strain: *Limnohabitans* lineages - LimB (strain Rim11) and LimA (Rim8); *Polynuclobacter* lineages - PnecC (two strains with identical rRNA sequences, czRimov8-C6 and czRimov-FAMC1) and PnecD (strain MoIso2); Met-TU (*M. turicensis*, strain MMS-10A-171); and Luna 2 cluster of *Actinobacteria* (strain MWH-Wo1). Significant differences between growth parameters of natural HNF communities growing on the different bacterial prey categories are shown in Supplemental information Table S2. Panels **b, d** and **f** show variability in the growth parameters for pooled data of all tested strains (ALL). Panel **b** shows also variability in growth rate of HNF communities growing in plankton samples from Římov reservoir filtered through 5 μm-pore-size filters (removal of HNF grazers) and incubated in dialysis bags in situ without any bacterial prey amendments (Dialbags, the blue boxplot presenting the data taken from Šimek et al. 2006, for details *see* the text).

Figure 4. Relationships between flagellate growth parameters with data pooled from all experiments (*see* Table 2) conducted with samples from Římov reservoir, Cep lake and with the *Poterioochromonas* sp. culture amended by different bacteria: (**a**) Gross growth efficiency (GGE) and maximum growth rate (**b**) related to length of the lag phase after the treatment was amended by different prey bacteria, and (**c**) GGE related to maximum growth rate fitted by linear regression. R^2 is the coefficient of determination of the regressions between the pairs of the parameters (n = 48). Bacterial strains affiliated to lineages LimA, LimB, LimC, PnecC, PnecD and the strains *Methylopumilus turicensis* (Met-TU) and MWH-Wo1 (Luna 2) were plotted separately in different symbols and colors. Note that the prey category LimC represents data gained with 9 different strains in 29 treatments (compare Fig. 3 and Table 1). Each data point represents the mean values from triplicate treatments. The data for the growth parameters of *Poterioochromonas* sp. on LimC and PnecD lineages are plotted as red symbols (Poterio-LimC and Poterio-PnecD) but they are involved in the overall regression analysis depicted in panels **a-c**.

Figure 5. Comparison of season-specific variability (experiments conducted in April, May, August, and October in Římov reservoir or Cep lake, for details *see* Table 2) in growth

responses of natural HNF communities amended by additions of the same prey group, i.e. Luna 2 cluster (strain MWH-Wo1), LimB lineage (strain Rim11), and the pooled data for the closely related strains belonging to LimC and PnecC lineages. Data variability is shown in box plots with $5^{th}/95^{th}$ percentile (full symbols are outliers, full line shows median value) of flagellate maximum growth rate (panels **a**–**d**), GGE (panels **e**–**h**), and lag phase (panels **i**–**l**). Overall, independent of the season, the data for the Luna 2 cluster (yellow bars) always differed significantly (Two-way ANOVA, Effective hypothesis decomposition, $p < 0.05$) in the growth parameters from other three bacterial prey categories. The season-specific significant differences (Unequal N HSD multiple comparison test, $p < 0.05$) in the HNF growth responses to the added prey items are indicated by capital letters on the top of panels (**e**–**l**); n.s. – not significant (panels **a**–**d**).

Figure 6. A general model based on the idea that major groups of both bacterioplankton and bacterivorous HNF have comparable growth potentials in pelagic systems. Panel **a** - the grey area represents relative growth balance between bacteria and bacterivorous HNF, yielding an approximate 1:1 ratio at which a relative stability of both bacterial and HNF community compositions and growth are assumed. The black text and arrows represent factors that may stimulate either bacterial or flagellate growth; the red text and red arrows represent factors leading to decreases in bacterial and flagellate growth (for details *see* the text). Panel **b** illustrates four model phases labeled as 1–4, with colors and sizes of drawings and circles indicating shifts in bacterial and flagellate cell and community sizes. Phase 1 – balance in relatively low growth of both bacteria and HNF. Phase 2 – a marked (e.g. bottom-up induced) bacterioplankton community shift towards rapidly growing bacterial species of large cell size, yielding a temporal imbalance in bacterial prey community and their grazers that results in low grazing control of the bacteria and short-lived bacterial peaks. Phase 3 – the bacterial outgrowth stimulates a flagellate predator population increase and its community shift, resulting in temporal re-establishment of the prey-predator balance at high growth rates. Phase 4 – resource limitation of the prevailing bacterial prey constrains bacterial population growth and thus further growing grazer populations decimate the bacteria and in consequence resource limitations and community shifts in both predator and prey assemblages are assumed. The arrow connecting phases 4 and 1 suggests re-establishment of the predator-prey balance at low growth rates at the original start of the model cycle. However, two bi-directional dashed arrows in the middle of the picture indicate that there are many transient stages from imbalance to temporal growth balance between the predator and prey

933 communities.

Table 1. Characteristics of bacterial strains used in this study.

Species, lineage affiliation	Strain	MCV ± SD (μm^3)	Cell shape	Origin	Reference	Experiment Identifier
LimA lineage, *Limnohabitans*, *Comamonadaceae*, *Betaproteobacteria*						
Limnohabitans sp.	Rim8	0.107 ± 0.008	Solenoid	Římov Reservoir, Czech Republic	Kasalický et al. 2013	XI
LimB lineage, *Limnohabitans*, *Comamonadaceae*, *Betaproteobacteria*						
Limnohabitans sp.	Rim11	0.056 ± 0.009	Short rod	Římov Reservoir, Czech Republic	Kasalický et al. 2013	II, VII, VIII, X
LimC lineage, *Limnohabitans*, *Comamonadaceae*, *Betaproteobacteria*						
Limnohabitans planktonicus	II-D5^T	0.162 ± 0.045	Large rod	Římov Reservoir, Czech Republic	Kasalický et al. 2010	IA, IB, II, III, IV, V, VI, VII, VIII
Limnohabitans parvus	II-B4^T	0.055 ± 0.006	Short rod	Římov Reservoir, Czech Republic	Kasalický et al. 2010	IA, IB, II, VII, VIII
Limnohabitans sp.	2KL-27	0.067 ± 0.038	Coccoid	Klíčava Reservoir Czech Republic	Kasalický et al. 2013	IA, IB
Limnohabitans sp.	2KL-1	0.204 ± 0.110	Large solenoid	Klíčava Reservoir Czech Republic	Kasalický et al. 2013	IA, IB
Limnohabitans sp.	2KL-3	0.548 ± 0.116	Large solenoid	Klíčava Reservoir Czech Republic	Kasalický et al. 2013	III, IV, V, VI
Limnohabitans sp.	T6-5	0.411 ± 0.045	Thin curved rod	Lužnice pond T6 Czech Republic	Kasalický et al. 2013	III, IV, V, VI, X
Limnohabitans sp.	Rim28	0.052 ± 0.013	Coccoid	Římov Reservoir,	Kasalický et al. 2013	II, VII, VIII

				Czech Republic		
Limnohabitans sp.	Rim47	0.080 ± 0.021	Coccoid	Římov Reservoir, Czech Republic	Kasalický et al. 2013	VII, VIII, X
Limnohabitans sp.	15K	0.054 ± 0.006	Ovoid	Římov Reservoir, Czech Republic	Kasalický et al. 2013	II
PnecC lineage, *Polynucleobacter*, *Burkholderiaceae, Betaproteobacteria*						
Polynucleobacter sp.	czRimov8-C6 *	0.058 ± 0.013	Small solenoid	Římov Reservoir,	- Undescribed	IX, X
	czRimov-FAMC1*	0.049 ± 0.010	Small solenoid	Czech Republic	- Undescribed	IX, X
PnecD lineage, *Polynucleobacter*, *Burkholderiaceae, Betaproteobacteria*						
Polynucleobacter cosmopolitanus	MWH-MoIso2^T	0.049 ± 0.023	Short curved rods	Lake Mondsee, Austria	Hahn et al. 2010	IA, IB
Methylopumilus*, *Methylophilaceae*, *Betaproteobacteria						
'Ca. Methylopumilus turicensis'	MMS-10A-171	0.042 ± 0.004	Short rod	Lake Zurich, Switzerland	Salcher et al. 2015	XI
Luna-2 subcluster, *Microbacteriaceae, Actinobacteria*						
Actinobacterium Undescribed	MWH-Wo1	0.061 ± 0.021	Small solenoid	Lake Wolfgangsee, Austria	Hahn and Pöckl 2005	IA, IB, II, XI.

* *Polynucleobacter* strains czRimov8-C6 and czRimov-FAMC1 share identical 16S rRNA gene sequences. MCV – mean cell volume;

Table 2. Overview and timing of bacterial prey manipulation experiments (numbered in bold) conducted in the Římov Reservoir and Lake Cep in different seasonal phases during the period 2011-2015. Main chemical and microbial parameters are shown for samples collected for the experiments.

Experiment/timing (In situ temperature)	Site Bacterivore	HNF (10^3 ml^{-1})	HNF MCV (μm^3)	Bacteria (10^6 ml^{-1})	Bacteria MCV (μm^3)	Chl-*a* (μg l^{-1})	TP (μg l^{-1})	DRP (μg l^{-1})	Bacterial strains used as prey
IA. 21.–24. 4. 2011 (15°C) *	Římov - HNF	0.967	12.4	4.496	0.043	11.5	33.8	1.2	II-D5^T, II-B4^T, 2KL-27, 2KL-1, MWH-MoIso2^T, MWH-Wo1
IB. 21.–24. 4. 2011 (cultured at 18°C)	*Poterio-ochromonas*	The same prey bacteria as in the experiment **IA** were fed to an axenic culture of *Poterioochromonas* sp.							II-D5^T, II-B4^T, 2KL-27, 2KL-1, MWH-MoIso2^T, MWH-Wo1
II. 10.–13. 10. 2011 (16°C)	Římov - HNF	0.658	15.5	3.944	0.056	10.2	28.2	6.7	II-B4^T, Rim11, Rim28, 15K, MWH-Wo1
III. 23.–27. 4. 2012 (16°C) ♦	Římov - HNF	3.529	26.7	2.79	0.094	11.6	26.9	11.6	II-D5^T, T6-5, 2KL-3
IV. 23–27 Apr 2012 (16°C) ♦	Cep - HNF	0.872	16.5	3.164	0.050	3.9	8.6	5.2	II-D5^T, T6-5, 2KL-3
V. 28.5. –1.6. 2012 (18°C) ♦	Římov - HNF	0.470	16.5	2.111	0.040	3.5	21.7	7.6	II-D5^T, T6-5, 2KL-3
VI. 28.5. –1.6. 2012 (19°C) ♦	Cep - HNF	0.371	8.9	1.531	0.041	3.1	10.0	5.7	II-D5^T, T6-5, 2KL-3
VII. 22.–25. 4. 2013 (15°C)	Římov - HNF	1.554	33.1	2.072	0.061	7.7	34.8	9.1	II-D5^T, II-B4^T, Rim11, Rim28, Rim47
VIII. 26–29. 8. 2013 (21°C)	Římov - HNF	1.345	22.1	3.522	0.056	8.9	20.5	3.1	II-D5^T, II-B4^T, Rim11, Rim28, Rim47
IX. 22.–26. 4. 2014 (16°C)	Římov - HNF	1.319	24.4	3.626	0.055	5.1	16.1	2.2	czRimov8-C6, czRimov-FAMC1
X. 18.–22. 8. 2014 (21°C)	Římov - HNF	1.236	24.6	2.960	0.067	12.1	19.9	3.8	czRimov8-C6, czRimov-FAMC1, Rim11, Rim47, T6-5,
XI. 25. –29. 5. 2015 (18°C)	Římov - HNF	1.795	32.3	2.054	0.061	5.7	16.3	1.8	Rim8, MWH-Wo1, MMS-10A-171

TP, total phosphorus; DRP, dissolved reactive phosphorus; Chl *a*, chlorophyll *a*; MCV, mean cell volume. * Selected data from the experiment IA have been used in the previous study (Šimek et al. 2013). ♦ Selected data from the experiments III-VI have been used also in the study of Grujčić et al. (2015).

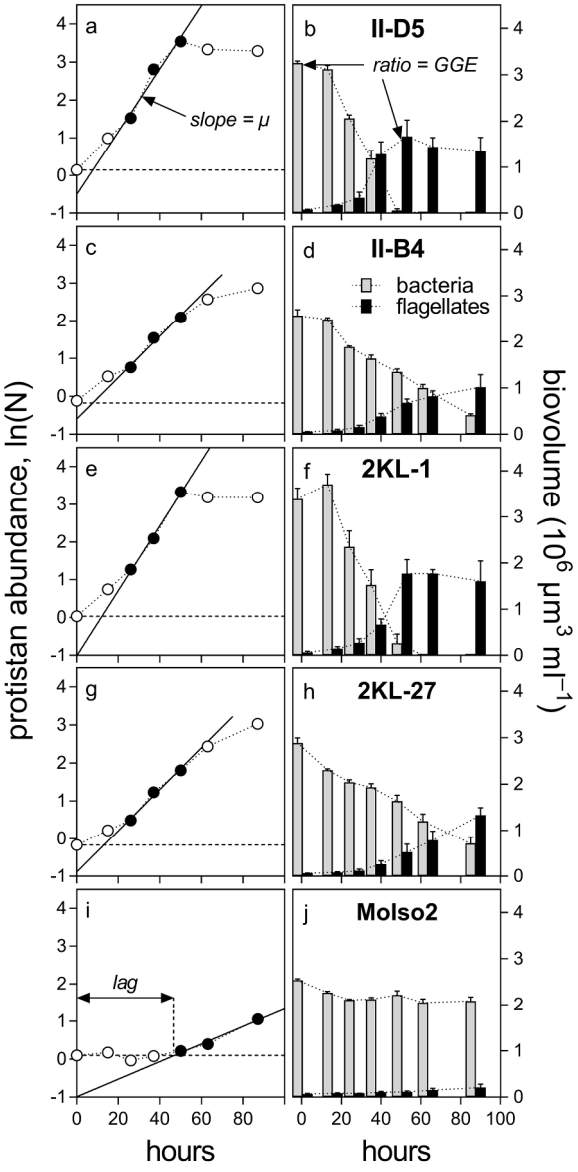

Figure 1. Examples of time course changes in abundance (a, c, e, g, i) and biovolume of the mixotrophic bacterivorous flagellate Poterioochromonas sp. in comparison to bacterial biovolume (b, d, f, h, j) in the treatments amended with respective bacterial strains in experiment IB (further details see in Tables 1 and 2). The arrows in panel b highlight the data points selected to calculate volumetric GGE values. Full symbols in panels a, c, e, g, and i highlight the time points selected to calculate the maximum flagellate growth rate (slope = μ, see the arrow in panel a). The length of lag phase was calculated as the period from the time zero to the intercept between the best-fit line of the flagellate growth and the zero-time level of its abundance as depicted in panel i. Values are means of triplicates; error bars show SD. Data for the strain MWH-Wo1 and control treatments are not shown as no flagellate growth was detected.

152x304mm (300 x 300 DPI)

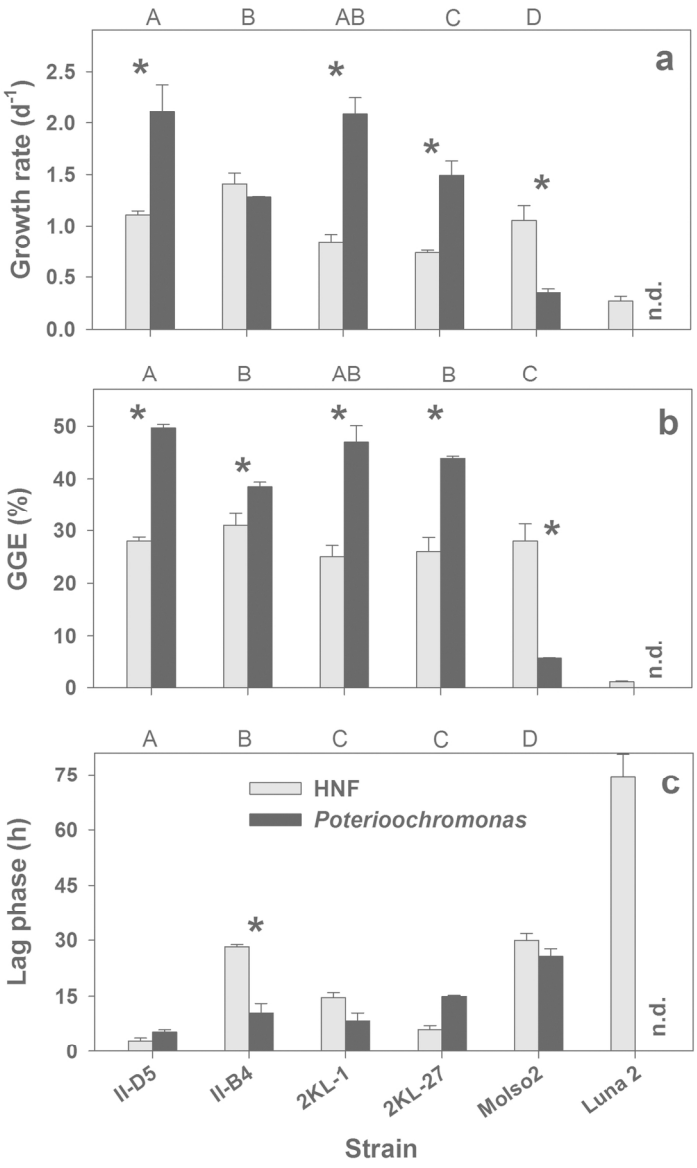

Figure 2. Growth parameters of HNF communities versus Poterioochromonas sp. Maximum growth rate (a), gross growth efficiency (GGE, b), and length of lag phase after the treatment amendment (c) of a natural planktonic HNF community (Římov reservoir) in comparison to a culture of the bacterivorous flagellate Poterioochromonas sp. amended by additions of the same biovolume of different bacterial prey. The prey bacteria were 4 strains of the genus Limnohabitans, i.e., L. planktonicus (II-D5), L. parvus (II-B4), 2KL-27 and 2KL-1, and the strains MoIso2 and Luna 2 (the MWH-Wo1 strain, for details see Tables 1 and 2). Values are means for triplicates; error bars show SDs. Different capital letters indicate a significant difference ($p < 0.05$, two-way ANOVA, followed by Unequal N HSD multiple comparison post-hoc test) between treatments amended with different bacterial strains. Stars above bars denote significant difference in the growth responses of the HNF community versus Poterioochromonas sp. growing on the same prey item. n.d. – no growth of Poterioochromonas on Wo1 was detected.

127x207mm (300 x 300 DPI)

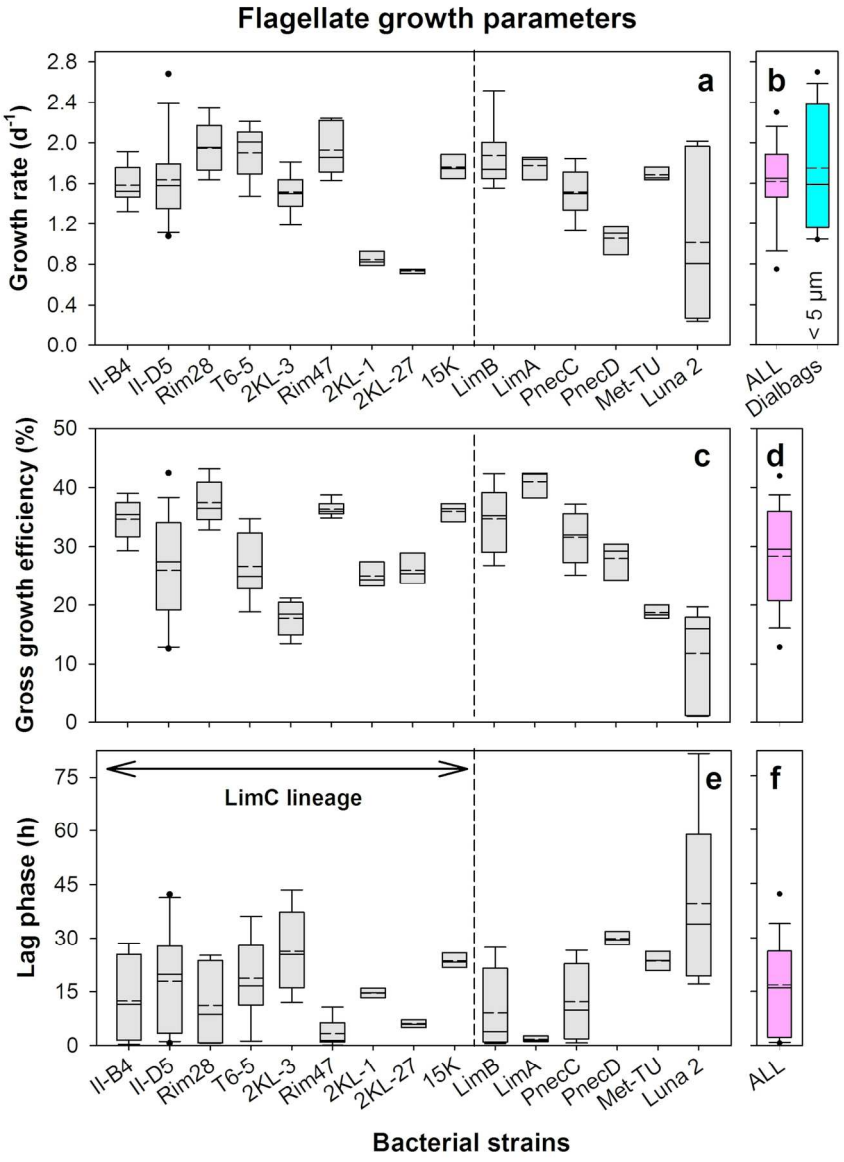

Figure 3. Overall variability in bacterial prey-specific responses across all experiments conducted with natural HNF communities from Římov reservoir and Cep Lake amended by additions of different bacterial strains. A total of 16 different bacterial strains were tested as HNF food, with some of them being used repeatedly during different plankton phases from April to October (for details see Table 1 and Fig. 5). Data variability of triplicate treatments in HNF maximum growth rate (a), volumetric GGE (c), and lag phase (e) are shown in box plots with 5th/95th percentile (full symbols are outliers, full and dashed lines, median and mean value, respectively). The box plots representing the data for bacterial strains labeled by the strain codes (Table 1), situated to the left of the vertical dashed line in panels a, c and e, are affiliated to the LimC lineage of the genus Limnohabitans. Other six prey categories plotted right side of the dashed line belong to different bacterial lineages and are largely represented by only one bacterial strain: Limnohabitans lineages - LimB (strain Rim11) and LimA (Rim8); Polynuclobacter lineages - PnecC (two strains with identical rRNA sequences, czRimov8-C6 and czRimov-FAMC1) and PnecD (strain MoIso2); Met-TU (M. turicensis, strain MMS-10A-171); and Luna 2 cluster of Actinobacteria (strain MWH-Wo1). Significant differences between

growth parameters of natural HNF communities growing on the different bacterial prey categories are shown in Supplemental information Table S2. Panels b, d and f show variability in the growth parameters for pooled data of all tested strains (ALL). Panel b shows also variability in growth rate of HNF communities growing in plankton samples from Římov reservoir filtered through 5 μm-pore-size filters (removal of HNF grazers) and incubated in dialysis bags in situ without any bacterial prey amendments (Dialbags, the blue boxplot presenting the data taken from Šimek et al. 2006, for details see the text).

152x210mm (300 x 300 DPI)

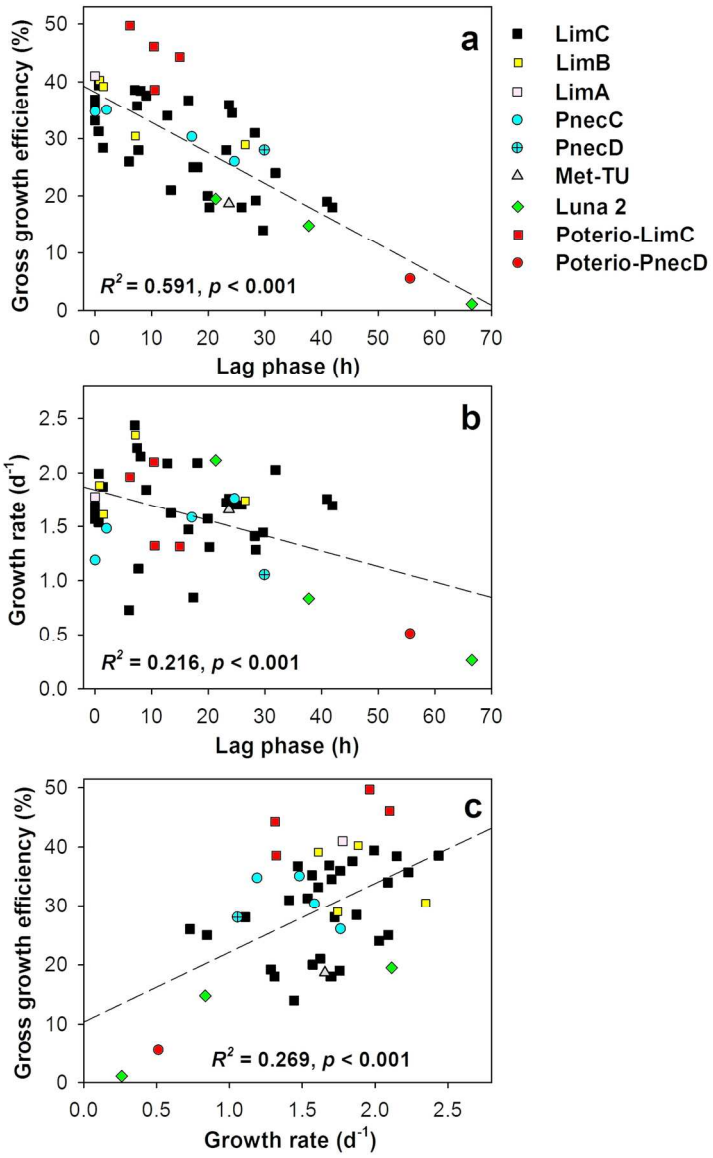

Figure 4. Relationships between flagellate growth parameters with data pooled from all experiments (see Table 2) conducted with samples from Římov reservoir, Cep lake and with the Poterioochromonas sp. culture amended by different bacteria: (a) Gross growth efficiency (GGE) and maximum growth rate (b) related to length of the lag phase after the treatment was amended by different prey bacteria, and (c) GGE related to maximum growth rate fitted by linear regression. R2 is the coefficient of determination of the regressions between the pairs of the parameters (n = 48). Bacterial strains affiliated to lineages LimA, LimB, LimC, PnecC, PnecD and the strains Methylopumilus turicensis (Met-TU) and MWH-Wo1 (Luna 2) were plotted separately in different symbols and colors. Note that the prey category LimC represents data gained with 9 different strains in 29 treatments (compare Fig. 3 and Table 1). Each data point represents the mean values from triplicate treatments. The data for the growth parameters of Poterioochromonas sp. on LimC and PnecD lineages are plotted as red symbols (Poterio-LimC and Poterio-PnecD) but they are involved in the overall regression analysis depicted in panels a-c.


138x217mm (300 x 300 DPI)

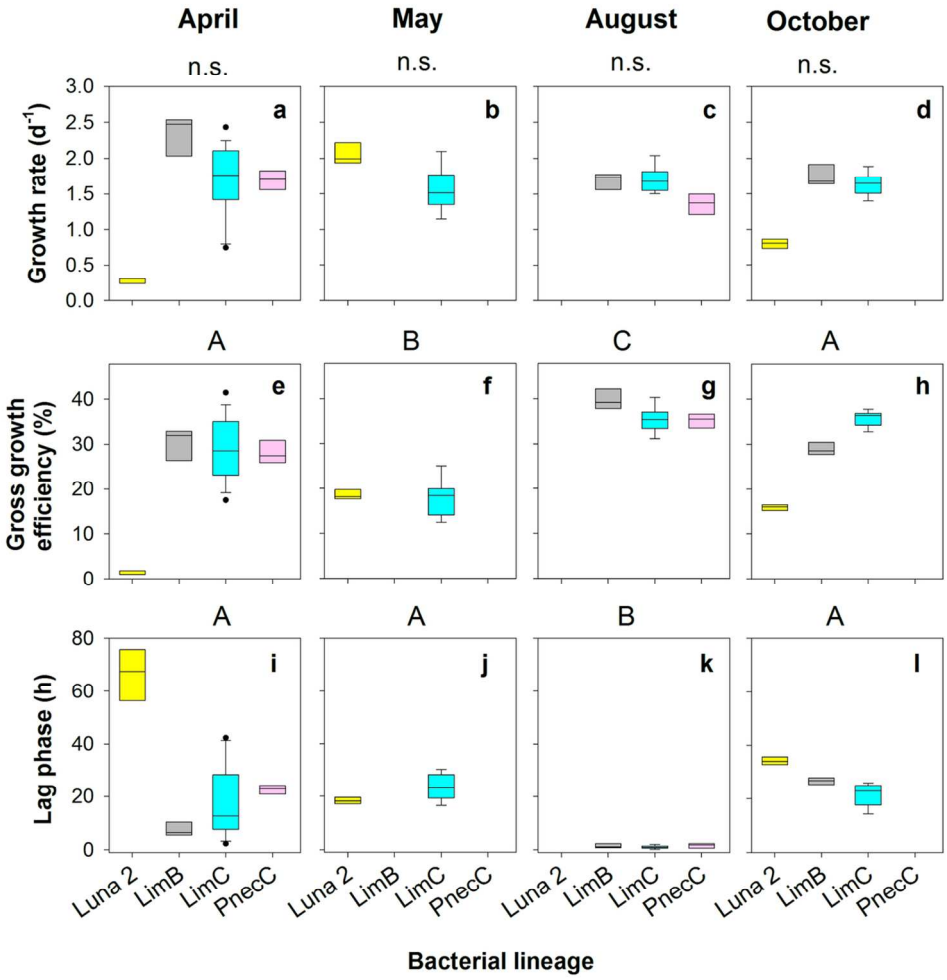

Figure 5. Comparison of season-specific variability (experiments conducted in April, May, August, and October in Římov reservoir or Cep lake, for details see Table 2) in growth responses of natural HNF communities amended by additions of the same prey group, i.e. Luna 2 cluster (strain MWH-Wo1), LimB lineage (strain Rim11), and the pooled data for the closely related strains belonging to LimC and PnecC lineages. Data variability is shown in box plots with 5th/95th percentile (full symbols are outliers, full line shows median value) of flagellate maximum growth rate (panels a–d), GGE (panels e–h), and lag phase (panels i–l). Overall, independent of the season, the data for the Luna 2 cluster (yellow bars) always differed significantly (Two-way ANOVA, Effective hypothesis decomposition, $p < 0.05$) in the growth parameters from other three bacterial prey categories. The season-specific significant differences (Unequal N HSD multiple comparison test, $p < 0.05$) in the HNF growth responses to the added prey items are indicated by capital letters on the top of panels (e–l); n.s. – not significant (panels a–d).

116x117mm (300 x 300 DPI)

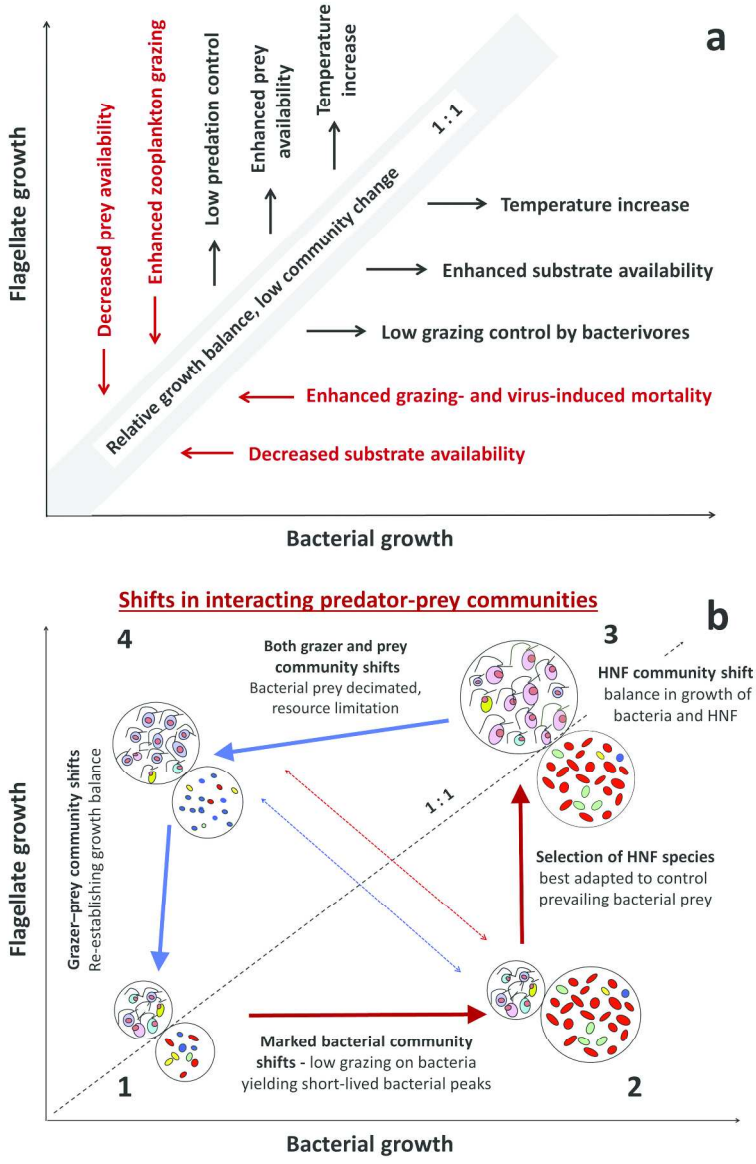

Figure 6. A general model based on the idea that major groups of both bacterioplankton and bacterivorous HNF have comparable growth potentials in pelagic systems. Panel a - the grey area represents relative growth balance between bacteria and bacterivorous HNF, yielding an approximate 1:1 ratio at which a relative stability of both bacterial and HNF community compositions and growth are assumed. The black text and arrows represent factors that may stimulate either bacterial or flagellate growth; the red text and red arrows represent factors leading to decreases in bacterial and flagellate growth (for details see the text). Panel b illustrates four model phases labeled as 1–4, with colors and sizes of drawings and circles indicating shifts in bacterial and flagellate cell and community sizes. Phase 1 – balance in relatively low growth of both bacteria and HNF. Phase 2 – a marked (e.g. bottom-up induced) bacterioplankton community shift towards rapidly growing bacterial species of large cell size, yielding a temporal imbalance in bacterial prey community and their grazers that results in low grazing control of the bacteria and short-lived bacterial peaks. Phase 3 – the bacterial outgrowth stimulates a flagellate predator population increase and its community shift, resulting in temporal re-establishment of the prey-predator balance at high growth rates.

Phase 4 – resource limitation of the prevailing bacterial prey constrains bacterial population growth and thus further growing grazer populations decimate the bacteria and in consequence resource limitations and community shifts in both predator and prey assemblages are assumed. The arrow connecting phases 4 and 1 suggests re-establishment of the predator-prey balance at low growth rates at the original start of the model cycle. However, two bi-directional dashed arrows in the middle of the picture indicate that there are many transient stages from imbalance to temporal growth balance between the predator and prey communities.

191x288mm (300 x 300 DPI)

Table 1. Characteristics of bacterial strains used in this study.

Species, lineage affiliation	Strain	MCV ± SD (μm^3)	Cell shape	Origin	Reference	Experiment Identifier
LimA lineage, *Limnohabitans*, *Comamonadaceae*, *Betaproteobacteria*						
Limnohabitans sp.	Rim8	0.107 ± 0.008	Solenoid	Římov Reservoir, Czech Republic	Kasalický et al. 2013	XI
LimB lineage, *Limnohabitans*, *Comamonadaceae*, *Betaproteobacteria*						
Limnohabitans sp.	Rim11	0.056 ± 0.009	Short rod	Římov Reservoir, Czech Republic	Kasalický et al. 2013	II, VII, VIII, X
LimC lineage, *Limnohabitans*, *Comamonadaceae*, *Betaproteobacteria*						
Limnohabitans planktonicus	II-D5^T	0.162 ± 0.045	Large rod	Římov Reservoir, Czech Republic	Kasalický et al. 2010	IA, IB, II, III, IV, V, VI, VII, VIII
Limnohabitans parvus	II-B4^T	0.055 ± 0.006	Short rod	Římov Reservoir, Czech Republic	Kasalický et al. 2010	IA, IB, II, VII, VIII
Limnohabitans sp.	2KL-27	0.067 ± 0.038	Coccoid	Klíčava Reservoir Czech Republic	Kasalický et al. 2013	IA, IB
Limnohabitans sp.	2KL-1	0.204 ± 0.110	Large solenoid	Klíčava Reservoir Czech Republic	Kasalický et al. 2013	IA, IB
Limnohabitans sp.	2KL-3	0.548 ± 0.116	Large solenoid	Klíčava Reservoir Czech Republic	Kasalický et al. 2013	III, IV, V, VI

Limnohabitans sp.	T6-5	0.411 ± 0.045	Thin curved rod	Lužnice pond T6 Czech Republic	Kasalický et al. 2013	III, IV, V, VI, X
Limnohabitans sp.	Rim28	0.052 ± 0.013	Coccoid	Římov Reservoir, Czech Republic	Kasalický et al. 2013	II, VII, VIII
Limnohabitans sp.	Rim47	0.080 ± 0.021	Coccoid	Římov Reservoir, Czech Republic	Kasalický et al. 2013	VII, VIII, X
Limnohabitans sp.	15K	0.054 ± 0.006	Ovoid	Římov Reservoir, Czech Republic	Kasalický et al. 2013	II
PnecC lineage, *Polynucleobacter*, *Burkholderiaceae, Betaproteobacteria*						
Polynucleobacter sp.	czRimov8-C6 *	0.058 ± 0.013	Small solenoid	Římov Reservoir,	- Undescribed	IX, X
	czRimov-FAMC1*	0.049 ± 0.010	Small solenoid	Czech Republic	- Undescribed	IX, X
PnecD lineage, *Polynucleobacter*, *Burkholderiaceae, Betaproteobacteria*						
Polynucleobacter cosmopolitanus	MWH-MoIso2^T	0.049 ± 0.023	Short curved rods	Lake Mondsee, Austria	Hahn et al. 2010	IA, IB
Methylopumilus*, *Methylophilaceae*, *Betaproteobacteria						
'Ca. Methylopumilus turicensis'	MMS-10A-171	0.042 ± 0.004	Short rod	Lake Zurich, Switzerland	Salcher et al. 2015	XI
Luna-2 subcluster, *Microbacteriaceae, Actinobacteria*						
Actinobacterium Undescribed	MWH-Wo1	0.061 ± 0.021	Small solenoid	Lake Wolfgangsee, Austria	Hahn and Pöckl 2005	IA, IB, II, XI.

* *Polynucleobacter* strains czRimov8-C6 and czRimov-FAMC1 share identical 16S rRNA gene sequences. MCV – mean cell volume;

Table 2. Overview and timing of bacterial prey manipulation experiments (numbered in bold) conducted in the Římov Reservoir and Lake Cep in different seasonal phases during the period 2011-2015. Main chemical and microbial parameters are shown for samples collected for the experiments.

Experiment/timing (In situ temperature)	Site Bacterivore	HNF (10^3 ml^{-1})	HNF MCV (μm^3)	Bacteria (10^6 ml^{-1})	Bacteria MCV (μm^3)	Chl-*a* (μg l^{-1})	TP (μg l^{-1})	DRP (μg l^{-1})	Bacterial strains used as prey
IA. 21.–24. 4. 2011 (15°C) *	Římov - HNF	0.967	12.4	4.496	0.043	11.5	33.8	1.2	II-D5^T, II-B4^T, 2KL-27, 2KL-1, MWH-MoIso2^T, MWH-Wo1
IB. 21.–24. 4. 2011 (cultured at 18°C)	*Poterio-ochromonas*	The same prey bacteria as in the experiment **IA** were fed to an axenic culture of *Poterioochromonas* sp.							II-D5^T, II-B4^T, 2KL-27, 2KL-1, MWH-MoIso2^T, MWH-Wo1
II. 10.–13. 10. 2011 (16°C)	Římov - HNF	0.658	15.5	3.944	0.056	10.2	28.2	6.7	II-B4^T, Rim11, Rim28, 15K, MWH-Wo1
III. 23.–27. 4. 2012 (16°C) ♦	Římov - HNF	3.529	26.7	2.79	0.094	11.6	26.9	11.6	II-D5^T, T6-5, 2KL-3
IV. 23–27 Apr 2012 (16°C) ♦	Cep - HNF	0.872	16.5	3.164	0.050	3.9	8.6	5.2	II-D5^T, T6-5, 2KL-3
V. 28.5. –1.6. 2012 (18°C) ♦	Římov - HNF	0.470	16.5	2.111	0.040	3.5	21.7	7.6	II-D5^T, T6-5, 2KL-3
VI. 28.5. –1.6. 2012 (19°C) ♦	Cep - HNF	0.371	8.9	1.531	0.041	3.1	10.0	5.7	II-D5^T, T6-5, 2KL-3
VII. 22.–25. 4. 2013 (15°C)	Římov - HNF	1.554	33.1	2.072	0.061	7.7	34.8	9.1	II-D5^T, II-B4^T, Rim11, Rim28, Rim47
VIII. 26–29. 8. 2013 (21°C)	Římov - HNF	1.345	22.1	3.522	0.056	8.9	20.5	3.1	II-D5^T, II-B4^T, Rim11, Rim28, Rim47
IX. 22.–26. 4. 2014 (16°C)	Římov - HNF	1.319	24.4	3.626	0.055	5.1	16.1	2.2	czRimov8-C6, czRimov-FAMC1
X. 18.–22. 8. 2014 (21°C)	Římov - HNF	1.236	24.6	2.960	0.067	12.1	19.9	3.8	czRimov8-C6, czRimov-FAMC1, Rim11, Rim47, T6-5,
XI. 25. –29. 5. 2015 (18°C)	Římov - HNF	1.795	32.3	2.054	0.061	5.7	16.3	1.8	Rim8, MWH-Wo1, MMS-10A-171

TP, total phosphorus; DRP, dissolved reactive phosphorus; Chl *a*, chlorophyll *a*; MCV, mean cell volume. * Selected data from the experiment IA were used in the previous study of Šimek et al. (2013). ♦ Selected data from the experiments III-VI were used in the previous study of Grujčić et al. (2015).

Supplemental Information, K. Šimek et al.

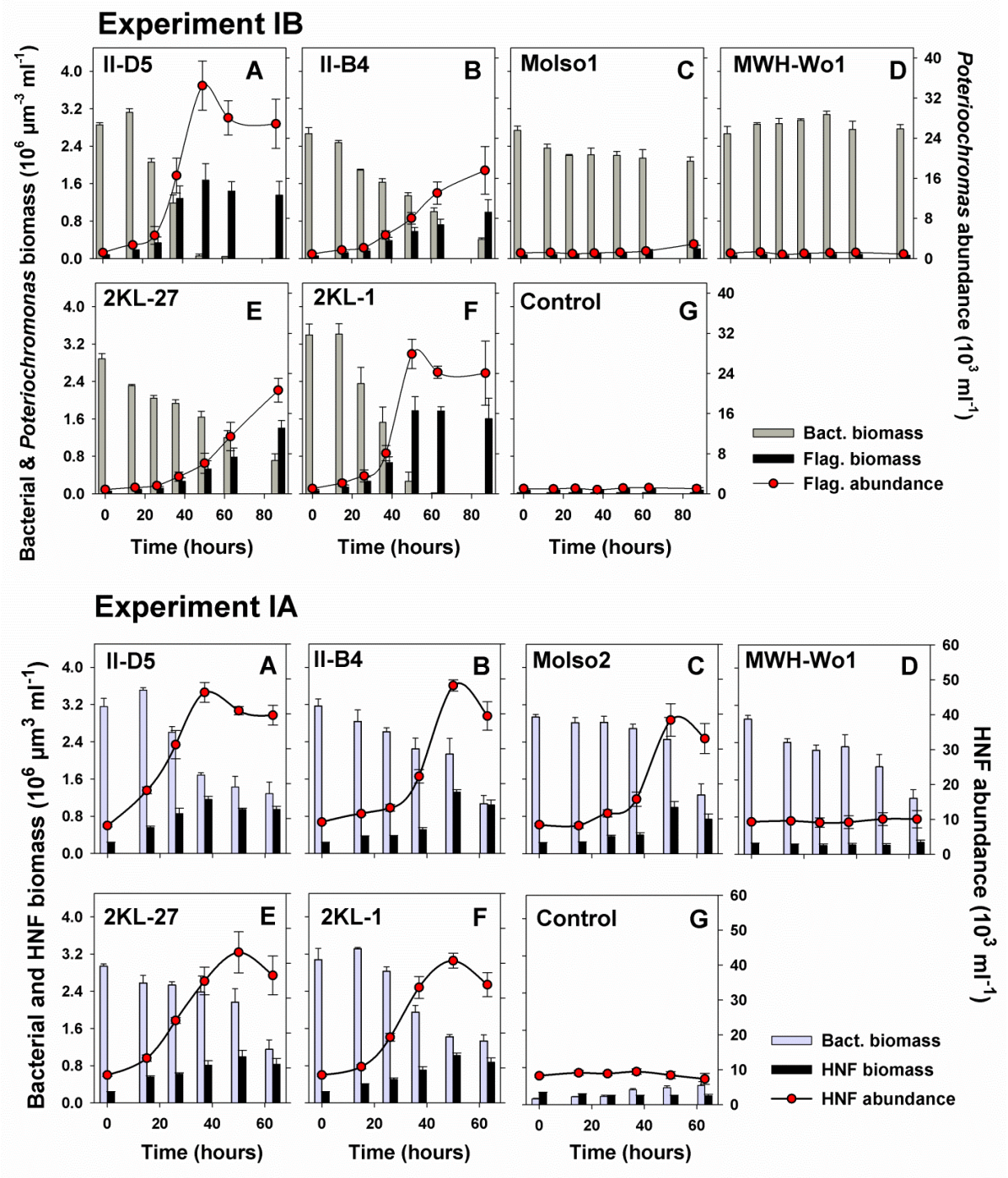

Supplemental Information, Figure S1. Note that the same experimental design and prey amendments were applied in Experiment IA and IB conducted in April 2011. Time-course changes in HNF abundance (Experiment IA) and *Poteroochromonas* sp. flagellate predator abundance and biovolume compared to bacterial biovolume in the treatments amended with respective bacterial strains (**A–F**, for details of the experimental timing and the bacterial strains used *see* Tables 1 and 2) compared with control (**G**) with no bacteria added. Values are means for triplicates; error bars show SD.

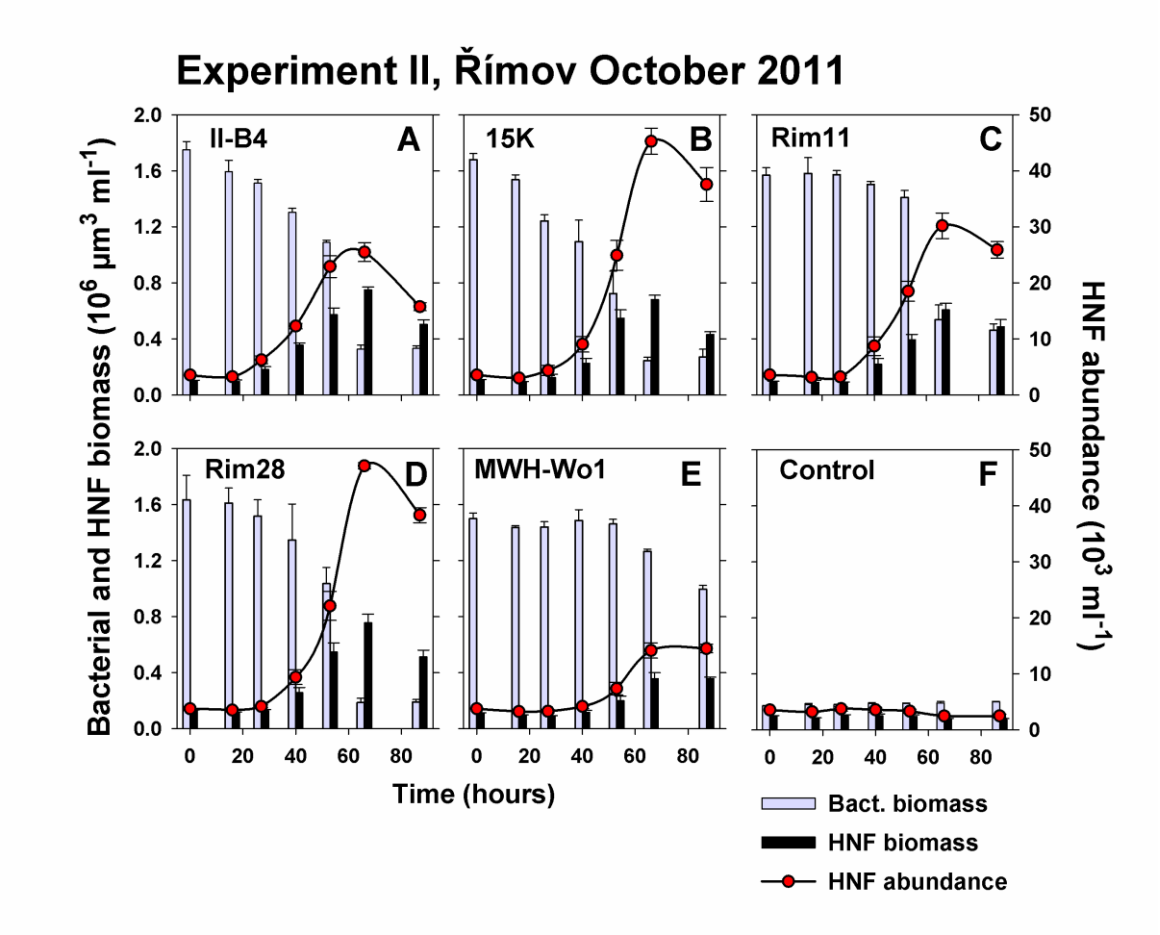

Supplemental Information, Figure S2. Expriment II conducted in October 2011. Time-course changes in HNF abundance and biovolume compared to bacterial biovolume in the treatments amended with respective bacterial strains (**A–E**, for details of the experimental timing and the bacterial strains used *see* Tables 1 and 2) compared with control (**F**) with no bacteria added. Values are means for triplicates; error bars show SD.

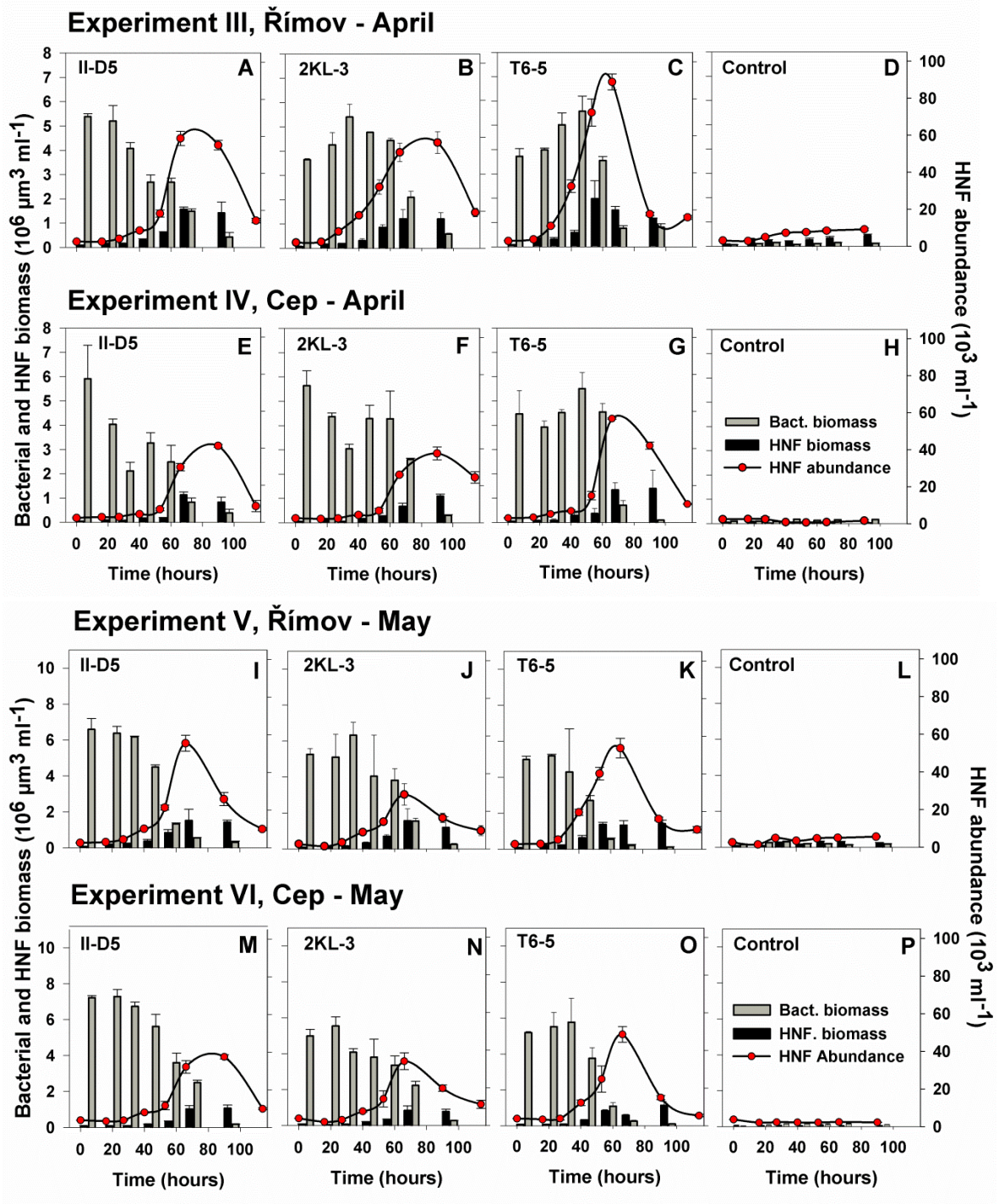

Supplemental Information, Figure S3. Experiments III-VI conducted in 2012. Time course changes in HNF abundance and volume biomass, compared to bacterial volume biomass in all treatments compared to controls, with all the experimental treatments being amended with the same strains (for details of the experimental timing and the bacterial strains used *see* Tables 1 and 2). **Experiment III**, Římov reservoir in April (**A to D**); **Experiment IV,** lake Cep in April (**E to H**); **Experiment V**, Římov reservoir in May (**I to L**); **Experiment VI,** lake Cep in May (**M to P**). Values are means of triplicates; error bars show SD.

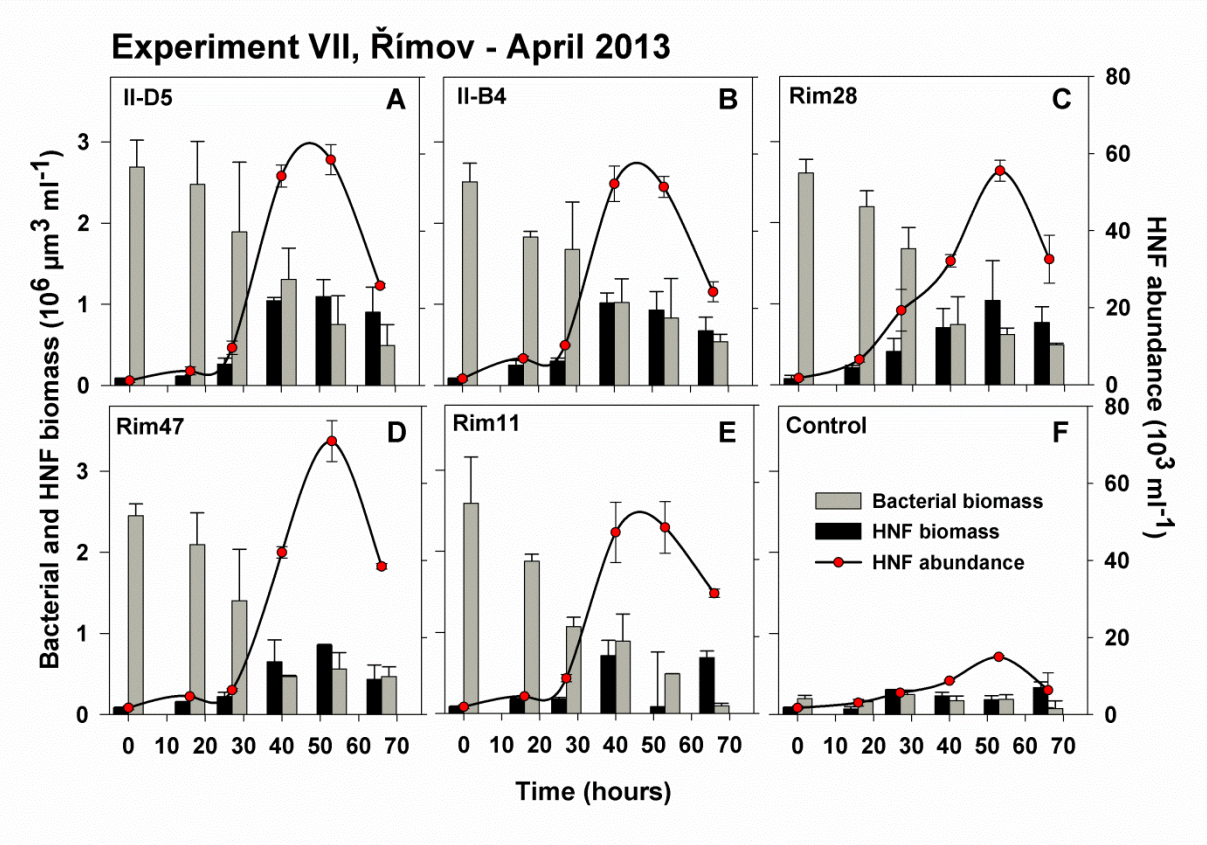

Supplemental Information, Figure S4. Experiment VII conducted in April 2013. Time-course changes in HNF abundance and biovolume compared to bacterial biovolume in the treatments amended with respective bacterial strains (**A–E**, for details of the experimental timing and the bacterial strains used *see* Tables 1 and 2) compared with control (**F**) with no bacteria added. Values are means for triplicates; error bars show SD.

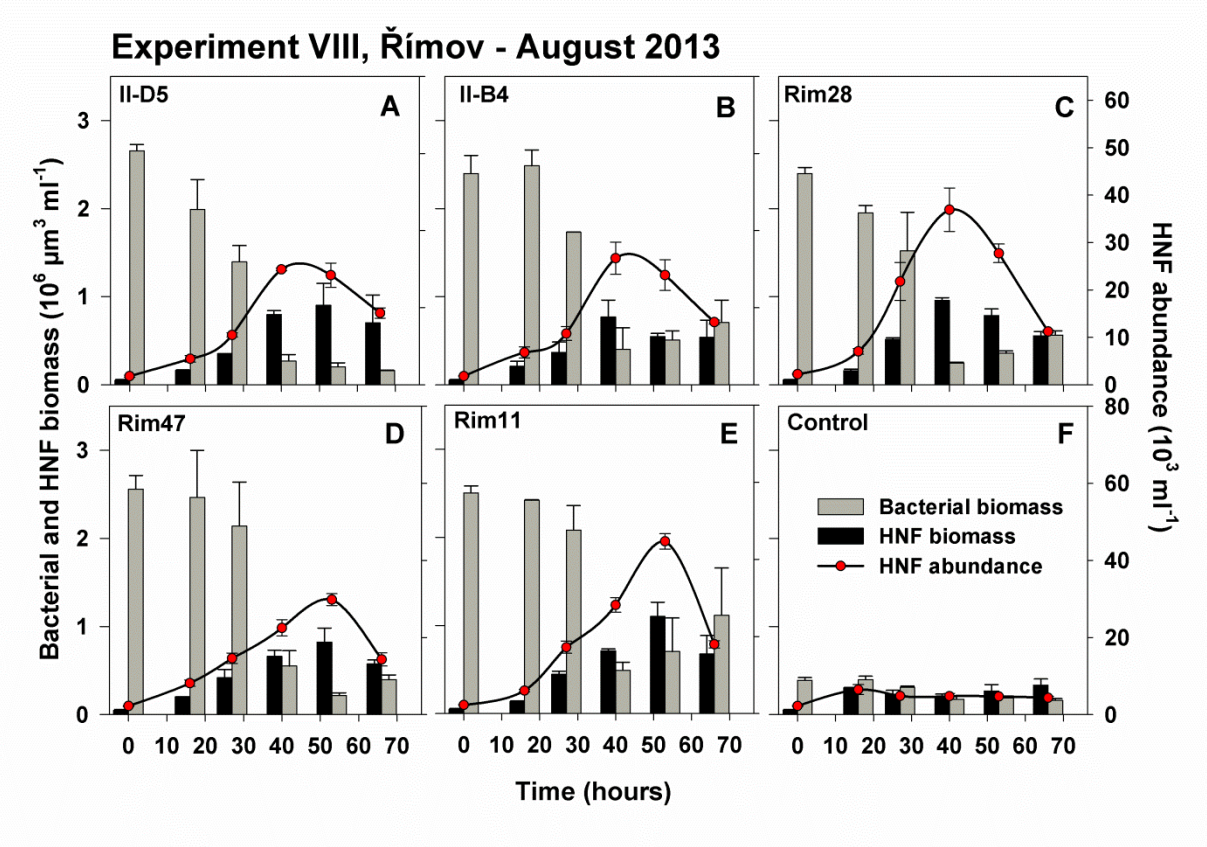

Supplemental Information, Figure S5. Experiment VIII conducted in August 2013. Time-course changes in HNF abundance and biovolume compared to bacterial biovolume in the treatments amended with respective bacterial strains (**A–E**, for details of the experimental timing and the bacterial strains used *see* Tables 1 and 2) compared with control (**F**) with no bacteria added. Values are means for triplicates; error bars show SD.

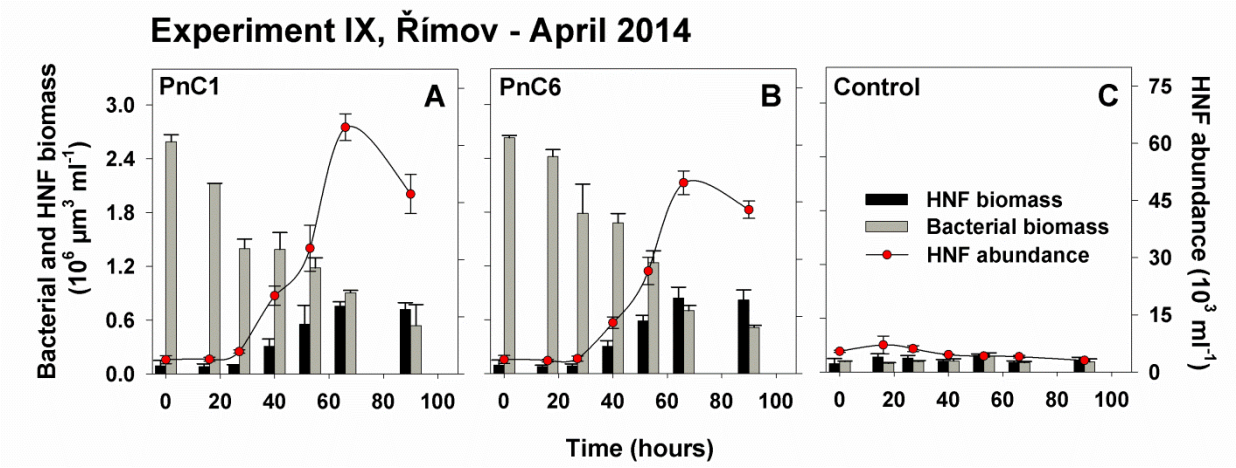

Supplemental Information Figure S6. Experiment IX conducted in April 2014. Time-course changes in HNF abundance and biovolume compared to bacterial biovolume in the treatments amended with respective bacterial strains (**A–B**, for further details *see* Tables 1 and 2) compared with control (**C**) with no bacteria added. Values are means for triplicates; error bars show SD.

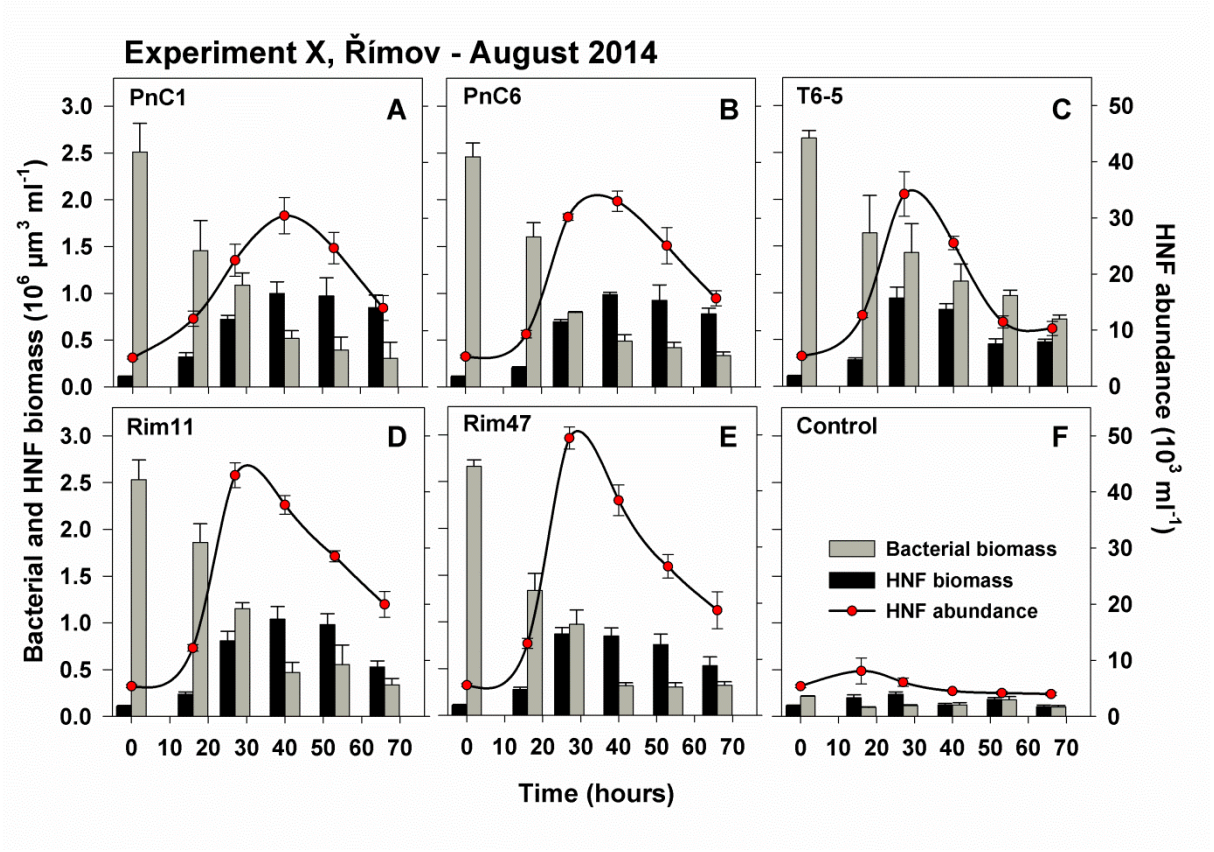

Supplemental Information Figure S7. Experiment X conducted in August 2014. Time-course changes in HNF abundance and biovolume compared to bacterial biovolume in the treatments amended with respective bacterial strains (**A–E**, for further details *see* Tables 1 and 2) compared with control (**F**) with no bacteria added. Values are means for triplicates; error bars show SD.

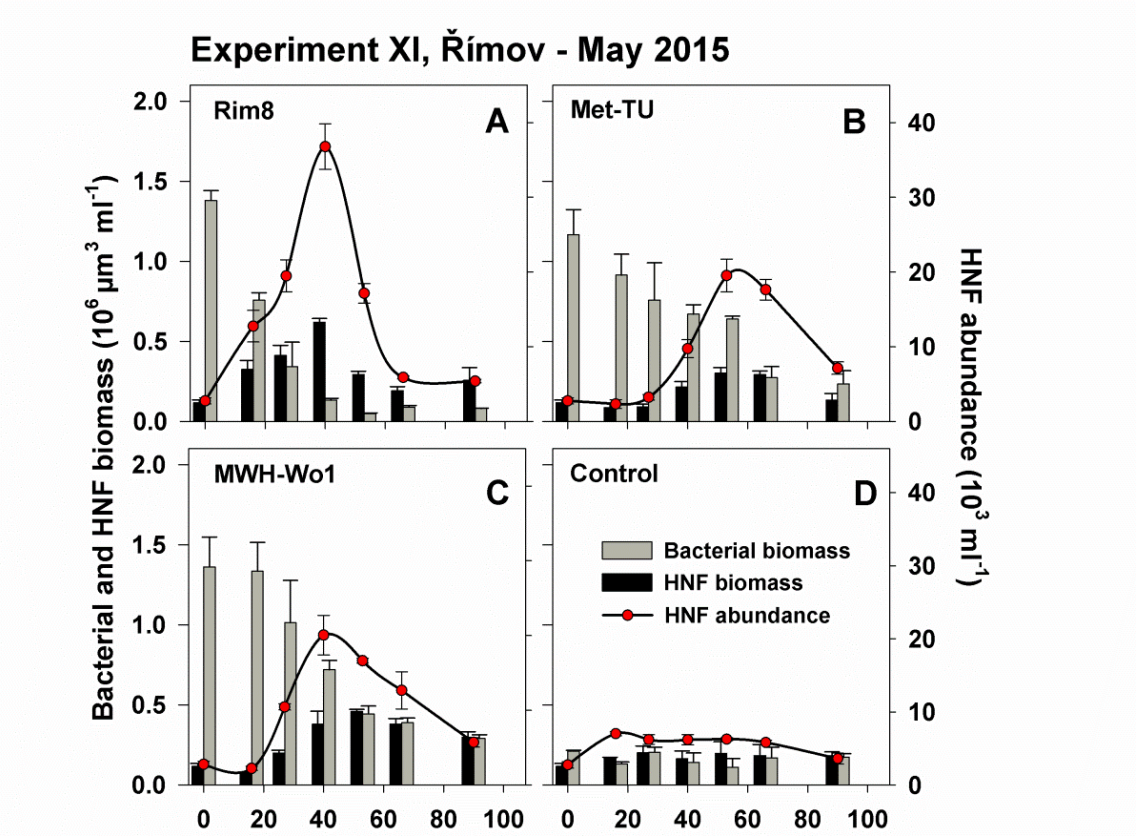

Supplemental Information Figure S8. Experiment XI conducted in May 2015. Time-course changes in HNF abundance and biovolume compared to bacterial biovolume in the treatments amended with respective bacterial strains (**A–C**, for further details *see* Tables 1 and 2) compared with control (**D**) with no bacteria added. Values are means for triplicates; error bars show SD.

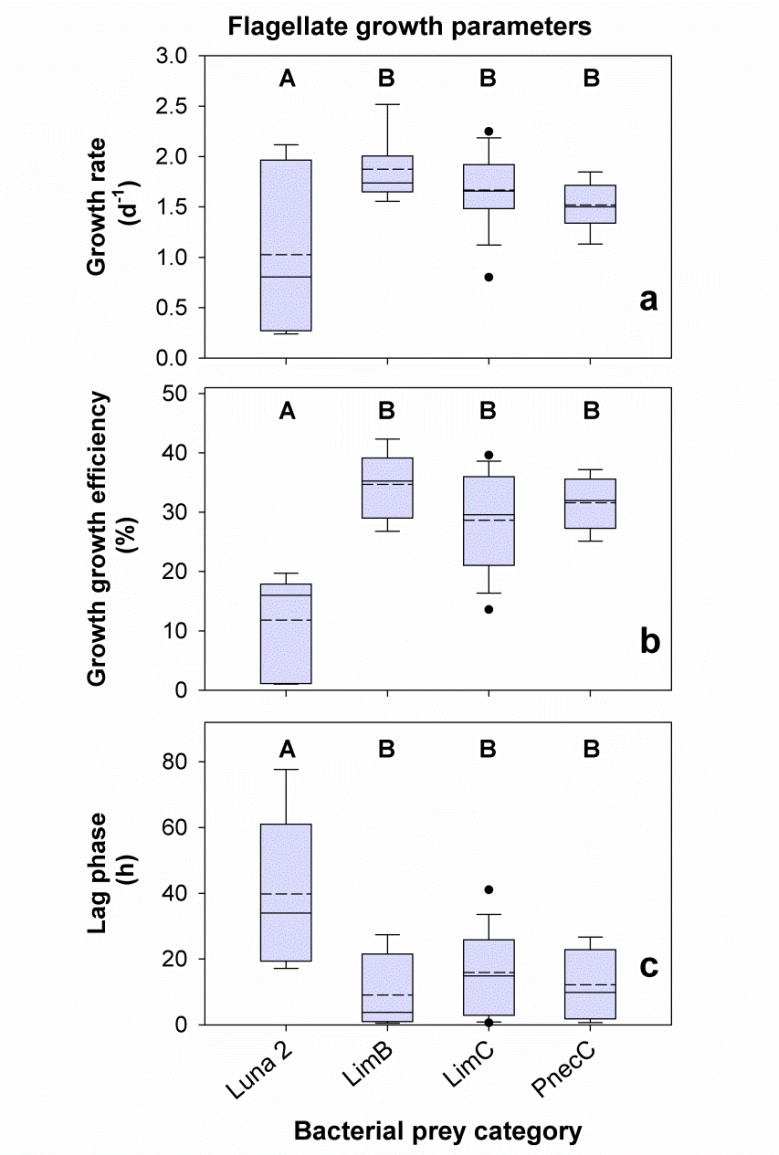

Supplemental Information Figure S9. Comparison of variability in growth responses of natural HNF communities from Římov Reservoir or Lake Cep to additions of the prey belonging to the same category independent on seasonal phase at which the experiments were conducted (for details *see* Table 2). The data representing 4 phylogenetically distinct prey categories were lumped together: (i) the Luna 2 cluster (represented only by the strain MWH-Wo1), (ii) LimB lineage (represented only by the strain Rim11), and the pooled data for closely related strains belonging to LimC and PnecC lineages (*see* Table 1). Data variability is shown in box plots with 5^{th}/95^{th} percentile (full symbols are outliers, full and dashed lines, median and mean value, respectively) of HNF maximum growth rate (**a**), GGE (**b**), and lag phase (**c**). The data for the strain from the Luna 2 cluster significantly differed (ANOVA, followed by Unequal N HSD multiple comparison post-hoc test, $p < 0.05$) in all growth parameters from other three bacterial prey categories as indicated by different capital letters.

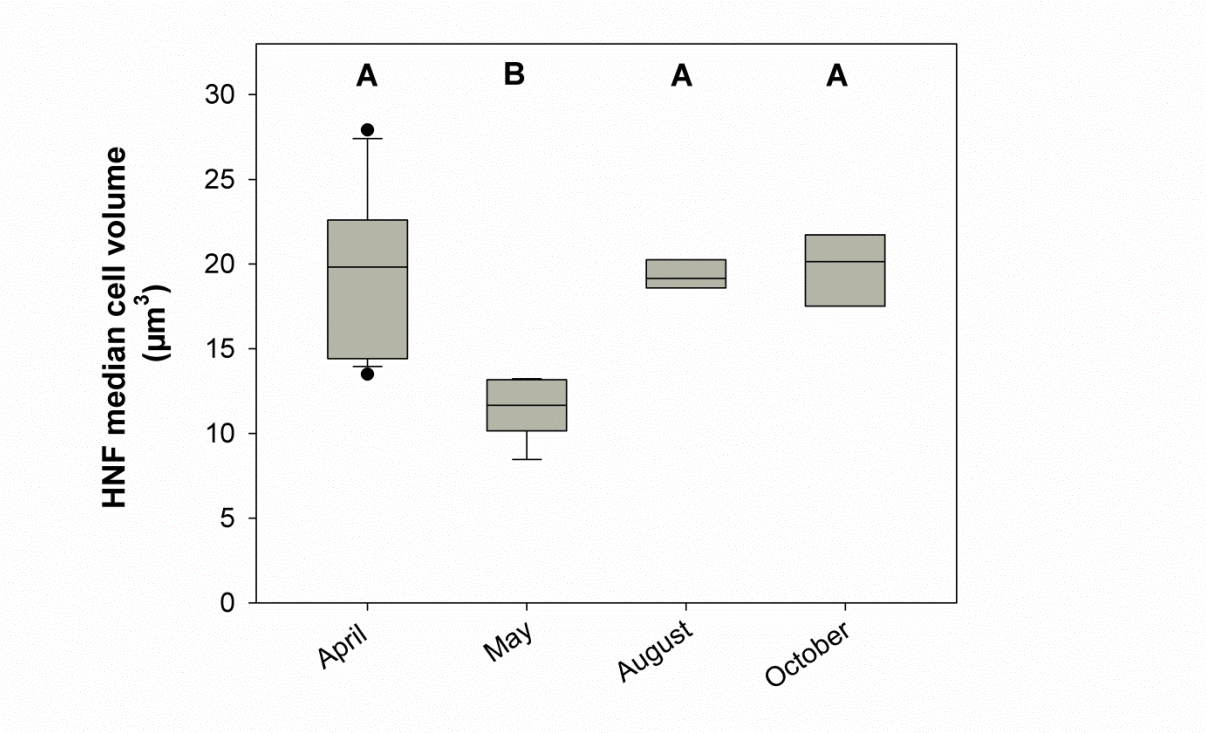

Supplemental Information Figure S10. Comparison of distribution of median values of flagellate cell volumes at samples taken for experiments conducted in April, May, August, and October. Data variability is shown in box plots with 5^{th}/95^{th} percentile, full symbols are outliers. Different capital letters indicate a significant difference ($p < 0.05$, one-way ANOVA, followed by Dunn's multiple comparison test) in median values between the different months.

Supplemental Information Table S1. Number (#) of treatments used to test statistical differences (Two-way ANOVA, Effective hypothesis decomposition followed by Unequal N HSD multiple comparison test) in growth responses of natural HNF communities to prey amendments with four different prey groups used in April, May, August, and October (significant differences shown in Figure 5). The prey groups represented **Luna 2** cluster (strain MWH-Wo1), **LimB** lineage (strain Rim11, *Limnohabitans*), and the pooled data for the closely related strains belonging to **LimC** (genus *Limnohabitans*) and **PnecC** lineages (genus *Polynucleobacter*; compare Tables 1 and 2). The data within each of the 4 prey groups were pooled to the season-specific data subsets from 9 and 2 experiments conducted with samples from the Římov reservoir (experiments IA, II,III, V, VII-XI) and Cep lake (experiments VI and VI), respectively (for details *see* Table 2).

	Luna 2 (# of treatments)	**LimB** (# of treatments)	**LimC** (# of treatments)	**PnecC** (# of treatments)
April	3	3	42	6
May	3	0	18	0
August	0	6	18	6
October	3	3	9	0

Supplemental Information Table S2: Significant differences (ANOVA followed with the Tukey post-test) between growth parameters of natural HNF communities growing on different bacterial strains shown in Fig. 3. Bacterial prey codes are compatible with the codes in Fig. 3, for details *see* the legend to Fig. 3.

	LimC, II-B4	LimC, II-D5	LimC, Rim28	LimC, T6-5	LimC, 2KL-3	LimC, Rim47	LimC, 2KL-1	LimC, 2KL-27	LimC, 15K	LimB	LimA	PnecC	PnecD	Met-TU	Luna2
LimC, II-B4															
LimC, II-D5															
LimC, Rim28															
LimC, T6-5															
LimC, 2KL-3	GGE***		GGE***												
LimC, Rim47					GGE***										
LimC, 2KL-1			µ***	µ***		µ***									
LimC, 2KL-27	µ***	µ*	µ***	µ***	µ*	µ***									
LimC, 15K					GGE***			µ*							
LimB					GGE***		µ***	µ***							
LimA		GGE**			GGE***		GGE*	µ*							
PnecC					GGE***			µ*							
PnecD			µ**	µ**		µ***				µ*					
Met-TU	GGE**		GGE***			GGE***		µ*	GGE*	GGE**	GGE***	GGE*			
Luna2	lag*** GGE***	GGE*	µ*** lag*** GGE***	µ*** GGE***		µ** lag*** GGE***	GGE*	lag** GGE*	GGE***	µ*** lag*** GGE***	lag*** GGE***	lag*** GGE***			

GGE, volumetric gross growth efficiency; µ, growth rate; probability: *, $p<0.05$; **, $p<0.01$, ***, $p<0.001$.